

https://dspace.org/

# Modelling the performance of Manganese electrowinning cells

**Rodrigues, Jose Carlos Pereira**

**2015**
http://hdl.handle.net/10539/19221

Downloaded from a DSpace repository. https://dspace.org/

# MODELLING THE PERFORMANCE OF MANGANESE ELECTROWINNING CELLS

José Carlos Pereira Rodrigues

A Dissertation Submitted to the Faculty of Engineering
University of the Witwatersrand , Johannesburg
for the Degree of Master of Science (Engineering)

Johannesburg 1983

DECLARATION

I, José Carlos Pereira Rodrigues, declare that this dissertation is my own work and has not been submitted to any other University

José Carlos P. Rodrigues

ACKNOWLEDGMENTS

I would like to dedicate this dissertation to my wife MARISA for her patience and perseverence throughout its duration

I would also like to thank
- my parents LÍGIA e JOÃO for their continuous and constant support throughout my educational carreer,
- my grandmother VIRGÍNIA for taking care of our daughter ANA MARA during our years of studying,
- my parents-in-law TELMA and CARLOS for their continuous assistance

In the academic field,I would like to thank
- Professor A.W. Bryson for his guidance and continuous help
- Dr. D.J. Pickett for his advice while he was at Wits
- the Chemical Engineering Department at Wits University as a whole
- last but not least Delta Manganese (Pty)Ltd for their assistance and for allowing me to use their plant data.

ABSTRACT

A comprehensive literature survey was conducted to obtain the available information on the manganese electrodeposition process.Using this information and measurments obtained from an industrial electrowinning plant,a model was developed where the interrelations between the most important parameters were taken into account.Fundamental concepts were used wherever possible,except in a small section where no theoretical data was available. In this case empirical fitting of parameters was resorted to.

The trends experienced in practice were all confirmed by the model,namely:

(i) the increase of cathodic current efficiency with increased pH,which is limited by the precipitation of manganese hydroxide:

(ii) the increased current efficiency with decreased ammonium sulphate concentration;

(iii) the existence of an optimum operating temperature for a given current density;

(iv) the existance of an optimum current density for a given temperature;

(v) the effect of total impurity level on current efficiency,the latter decreasing with increasing impurity level;

(vi) the steep increase of current efficiency with increase of feed flow rate,to an upper limit condition at which point manganese hydroxide starts precipitating.

LIST OF SYMBOLS

| | |
|---|---|
| $A$ | - submerged area of diaphragm ($m^2$) |
| $A_c$ | - area of cooling coils ($m^2$) |
| $B_j(x)$ | - concentration of jth species at position x ($kmole/m^3$) |
| $C^0_{pj}$, $C^*_{pj}$ | - molar and average molar specific heats of species j (kJ/kmole K) |
| $D_j$ | - diffusion coefficients of jth species ($m^2/s$) |
| $d$ | - diaphragm thickness (m) |
| $E^*_{oj}$ | - equilibrium potential when concentration of jth species is unity (V) |
| $E_a, E_c$ | - anode and cathode potentials (V) |
| $F$ | - Faraday's constant, 96500 (A.s/mol) |
| $H_j$ | - enthalpy of jth component (kJ/kmole) |
| $\Delta H^0_{fj}$ | - standard enthalpy of formation of jth species (kJ/kmole) |
| $\Delta H_{tj}$ | - enthalpy change due to the transformation from one phase to another (kJ/kmole) |
| $\Delta H'_j$ | - enthalpy correction due to non-ideal behaviour (kJ/kmole) |
| $h_1, h_2$ | - defined by equations (2.29) and (2.30) |
| $I$ | - total cell current (A) |
| $i, i_c, i_a$ | - current density at diaphragm, cathode and anode ($A/m^2$) |
| $i_j$ | - partial current density for jth reaction ($A/m^2$) |
| $i^*_{oj}$ | - exchange current density when concentration of jth component is unity |
| $K^*, K_c, K_a$ | - average, catholyte and anolyte conductivity (A/Vm) |
| $K$ | - equilibrium constant |
| $K'_c, K'_a, K'_s, K'_h$ | - defined by equations (2.2), (2.4), (2.6) and (2.9) |
| $k_j$ | - mass transfer coefficients of jth species (m/s) |

| | |
|---|---|
| $L_c, L_a$ | - distances between cathode and diaphragm and anode and diaphragm(m) |
| $L_{H_2Oc}, L_{H_2Oa}$, | - cathodic and anodic losses of water (kg/s) |
| $L_{NH_3}$ | - cathodic losses of ammonia (kg/s) |
| $M_j$ | - production rate of jth species,other than aqueous components(kmole/s) |
| $n_j$ | - number of electrons transferred in rate controlling step for jth component |
| $P_{Mn}, P_{O_2}, P_{H_2}$, $P_{MnO_2}$ | - production rates of manganese,oxygen, hydrogen,and manganese dioxide (kg/s) |
| $pH_f, pH_a, pH_c$ | - feed,anolyte and catholyte pH |
| $Q_f$ | - feed mass flowrate ($m^3/s$) |
| $Q_a$ | - discharge or anolyte flowrate($m^3/s$) |
| $Q_c$ | - cooling water flowrate($m^3/s$) |
| $Q_o$ | - flowrate of water through the diaphragm ($m^3/s$) |
| $q_c$ | - energy removed by the cooling coils (kJ/s) |
| $q_1$ | - energy correction term(kJ/s) |
| R | - ideal gas constant, 8,31(A.s/mol) |
| S | - total sulphate concentration in anolyte ($kmole/m^3$) |
| t,T | - temperature (°C),(K) |
| $T_a, T_c, T_1, T_2$ | - temperatures of anolyte,catholyte , cooling water in and out (K) |
| $\Delta T$ | - defined by equation(2.68) |
| V | - cell voltage (V) |
| $W_j$ | - diaphragm molar flow of jth species (kmole/s) |
| x | - distance into diaphragm from catholyte interface (m) |
| $y_j$ | - mole fraction of jth species in gas |
| $z_j$ | - charge on j+h species |

| | |
|---|---|
| $\Delta Y_1$ | - defined by equation (2.7) |
| $X_j, Y_j, Z_j$ | - concentration of aqueous species (kmole/m$^3$) see Table 4 |
| $\alpha_j$ | - defined by equation (2.14) |
| $\beta_j$ | - symmetry factor for jth component |
| $\gamma$ | - correlation coefficient in equation (2.32) |
| $\varepsilon$ | - diaphragm void fraction |
| $\lambda_j$ | - proportionality constants |
| $\eta$ | - voltage drop over catholyte, anolyte and diaphragm (V) |
| $\Phi$ | - fraction of plated surface containing impurity metals |
| $\mu_i$ | - electrochemical potential of species i |
| $\xi_c, \xi_a$ | - cathodic and anodic fractional current efficiencies |
| $\rho_f, \rho_a, \rho_c$ | - feed, anolyte and catholyte densities (kg/m$^3$) |

LIST OF FIGURES

Figure 1 - Simplified Flow Diagram of a Typical Industrial Manganese Production ..... 4
Figure 2 - Bottom Feed Cathode Frame Type Cell ..... 5
Figure 3 - Individual Side Discharge Type Cell ..... 6
Figure 4 - False Bottom Type Cell ..... 7
Figure 5 - False Bottom Type of Manganese Electro-winning Cell as used at Delta ..... 8
Figure 6 - Schematic Diagram of Cathode and Anode Frame with Diaphragm ..... 9
Figure 7 - Schematic Diagram of the Cooling Coils on a Cathode Frame ..... 10
Figure 8 - Sketch of the False-Bottom Side-Feed Cathode Frame Manganese Cell ..... 10
Figure 9 - Logic Diagram ..... 23
Figure 10 - Effect of Cathodic Current Density ..... 35
Figure 11 - Effect of Catholyte Temperature ..... 35
Figure 12 - Effect of Impurity Concentration ..... 36
Figure 13 - Flow Diagram for Mass Balance ..... 42
Figure 14 - Effect of Feed Flowrate ..... 49
Figure 15 - Fractional Current Efficiency versus Catholyte pH ..... 51
Figure 16 - Influence of pH on Current Efficiency as published by MINTEK(6) ..... 52
Figure 17 - Fractional Current Efficiency versus Ammonium Sulphate Concentration ..... 54
Figure 18 - Fractional Current Efficiency versus Total Impurity Level ..... 56
Figure 19 - Fractional Current Efficiency versus Feed Temperature ..... 58
Figure 20 - Fractional Current Efficiency versus Cathodic Current Density ..... 60
Figure 21 - Limiting Catholyte pH versus Ammonium Sulphate Concentration ..... 62

Figure 22 - Comparison Between Experimental Values and Model Values for the Equilibrium Ratio of the Manganese-Ammonia Complex Formation ..... 90
Figure 23 - Comparison between Reported and Model Values for the Ammonium-Ammonia Reaction Equilibrium Ratio ..... 92
Figure 24 - Equilibrium Ratio for the Precipitation of Manganese Hydroxide ..... 95
Figure 25 - The Sulphate-Bisulphate Equilibrium Ratio as a function of Temperature-Model Predictions ..... 97
Figure 26 - Fitting the Impurity Model .....107
Figure 27 - Fitting the Current Density Effect .....108
Figure 28 - Fitting the Temperature Effect .....111
Figure 29 - Comparison Between Experimental Results and Model Predictions for the Mole Fraction versus Temperature in the Estimation of Water Losses .....113

LIST OF TABLES

Table 1 - Characteristic Composition of Cell Feed Solution ..... 12
Table 2 - Maximum Levels of Impurities in Cell Feed Solution ..... 13
Table 3 - Typical Analysis of Electrolytic Manganese ..... 13
Table 4 - Nomenclature of Aqueous Species ..... 25
Table 5 - Molar Enthalpies of Formation and Molar Specific Heats ..... 45
Table 6 - Typical Model Results ..... 47
Table 7 - Fractional Current Efficiency versus Feed Flowrate ..... 48
Table 8 - Fractional Current Efficiency versus Catholyte pH ..... 50
Table 9 - Ammonium Sulphate Concentration versus Fractional Current Efficiency ..... 53
Table 10 - Fractional Current Efficiency versus Total Impurity Concentration ..... 55
Table 11 - Fractional Current Efficiency versus Temperature ..... 57
Table 12 - Cathodic Current Density versus Fractional Current Efficiency ..... 59
Table 13 - Limiting Catholyte pH versus Ammonium Sulphate Concentration ..... 61
Table 14 - Feed Input - Mass Balance ..... 70
Table 15 - Products - Mass Balance ..... 71
Table 16 - Losses - Mass Balance ..... 72
Table 17 - Anolyte Discharge - Mass Balance ..... 74
Table 18 - Summary of the Overall Mass Balance..... 75
Table 19 - Energy Input in the Feed Stream ..... 85
Table 20 - Energy Output through the Discharge Stream ..... 86

Table 21 - Energy Term from Products and Losses ..... 87
Table 22 - Overall Energy Balance ..... 88
Table 23 - Experimental and Model Values for the Manganese-Ammonia Complex Reaction Equilibrium Ratio ..... 89
Table 24 - Experimental and Model Values for the Ammonium-Ammonia Equilibrium Ratio ..... 91
Table 25 - Experimental and Predicted Values for the Manganese Hydroxide Formation Reaction Equilibrium Ratio ..... 94
Table 26 - Fitting the Current Density Effect on the Kinetic Model .....109
Table 27 - Fitting the Temperature Effect .....110
Table 28 - Fitting the Mole Fraction Equation from Steam Tables (23) .....112

CONTENTS


1 - INTRODUCTION ..... 1

1.1 - The Production of Electrolytic Manganese ... 2

1.2 - The Manganese Electrowinning Cell ..... 3

1.2.1 - Cell Design Considerations ..... 5

1.2.3 - Cathodic Manganese Deposition ..... 11

1.2.3 - Choice of Electrodes ..... 11

1.2.4 - Characteristic Operatin Conditions .... 12

1.3 - Effects of Parameters on the Manganese Electrodeposition Process ..... 14

1.3.1 - Manganese Sulphate Concentration ..... 15

1.3.2 - Ammonium Sulphate Concentration ..... 15

1.3.3 - The Addition of Sulphur Compounds ..... 16

1.3.4 - Solution Temperature ..... 17

1.3.5 - The Current Density ..... 18

1.3.6 - The Solution pH ..... 18

1.3.7 - Impurities ir the Catholyte ..... 19

1.4 - The Modelling Exercise ..... 20

1.4.1 - Statistical Approach ..... 20

1.4.2 - Mechanistic Approach ..... 21

2 - MODEL COMPONENTS ..... 22

2.1 - Logistic of the Model ..... 22

2.2 - Solution Equilibria ..... 24

2.2.1 - Feed and Catholyte Equilibrium ..... 26

2.2.2 - Anolyte Equilibrium ..... 28

2.3 - Diaphragm Model ..... 29

2.4 - Kinetic Model ..... 31

2.4.1 - Cathodic Kinetic Model ..... 31

2.4.2 - Anodic Kinetic Model ..... 37

2.5 - Cell Voltage Model ..... 38

2.6 - Water Vapour and Ammonia Losses ..... 39

2.7 - Mass Balance ..... 41

2.8 - Energy Balance ..... 44

3 - RESULTS AND CASE STUDIES ..... 47
3.1 - Typical Results - Discussion ..... 47
3.2 - Case Studies ..... 48
3.2.1 - The Effect of Feed Flowrate on Fractional Current Efficiency ..... 48
3.2.2 - Effect of pH on Fractional Current Efficiency ..... 50
3.2.3 - The Influence of Ammonium Sulphate .... 53
3.2.4 - The Effect of Total Impurity Level on Fractional Current Efficiency ..... 55
3.2.5 - The Effect of Feed Temperature on Fractional _urrent Efficiency ..... 57
3.2.6 - The Effect of Cathodic Current Density on Fractional Current Efficiency ..... 59
3.2.7 - The Limiting Catholyte pH versus Ammonium Sulphate Concentration ..... 61

4 - REFERENCES ..... 63

APPENDICES

A - Computer Model ..... 67
B - Typical Mass Balance Calculations ..... 70
B.1 - Solving for the Feed Ion Concentrations .... 77
B.2 - Solving for the Anolyte Ion Concentrations . 81
C - Typical Energy Balance Calculation ..... 84
D - Solution Equilibrium Ratios ..... 89
D.1 - The Formation Of the Manganese-Ammonia Complex ..... 89
D.2 - The Ammonia-Ammonium Reaction ..... 91
D.3 - The Precipitation of Manganese Hydroxide ... 93
D.4 - The Sulphate-Bisulphate Equilibrium ..... 96
E - Theory on the Development of the Diaphragm Model. 98
F - Fitting the Cathodic Kinetic Model ..... 105
G - Water Losses - Modelling ..... 112

## 1. INTRODUCTION

South Africa is the largest producer of electrolytic manganese in the world.Over 90°/₀ of the metal produced from its two plants is exported.

The metal has many important uses,the main ones being in the steel and alumimium industries.Manganese is added to all grades of steel and acts as a deoxidiser and a desulphuriser .It stabilizes the austenitic phase at high temperatures and can replace part of the nickel content of stainless steel.It also decreases the carbon content of the steel ,giving it a greater toughness and fluidity (1).It is found that if manganese is added in a pure state steel properties are improved(2).Producers of low carbon and high manganese steels prefer the use of electrolytic manganese because of its high purity and simplification of the process required.

The other main consumer of electrolytic manganese is the aluminium industry.If manganese is added to aluminium alloys,it improves their mechanical,thermal and corrosion resistance properties .Iron and other impurities have to be carefully controlled to avoid the formation of hard spots when the aluminium slabs are being shaped.

Other smaller industrial uses of manganese are in the production of alloys of various non-ferrous metals such as manganese-magnesium and manganese-bronze,which display some important electric and magnetic properties.Copper-manganese alloys are also produced industrially as they show extremely high strength qualities,with applications in ship propellers,valves,nuts and bolts.Special ferrous super-alloys are used in jet engines,marine turbines and in nuclear energy industry.Some non-metallurgical applications of electrolytic manganese are in dry cell bat-

teries in the form of manganese dioxide,in paint and varnish driers,ceramic products,fungicides and pharmaceuticals.

## 1.1 - The Production of Electrolytic Manganese

In 1927 various processes of producing pure manganese were tested.In 1936,cathodic manganese was produced for the first time with 99.85% purity and an average current efficiency of 54%(2).Today electrolytic manganese is produced on a continuous basis from manganese ores through an electrowinning process using diaphragm cells(3).The manganese ore is ground to a powder prior to the reduction to a soluble form in a rotary kiln.It changes from the Manganese(III) and Manganese (IV) to the Manganese(II) state at temperatures of the order of 900°C.The reducing agent used is Carbon,which allows the manganese to be preferentially reduced to Manganese(II)oxide.During this reaction the bulk of the iron is left in a form that is insoluble to dilute sulphuric acid.In the leach section, the anolyte solution from the cell house and the reduced ore are mixed under controlled conditions,in order to maintain the pH between 5.2 and 6.2.This minimizes the dissolution of iron and other impurities such as silica, zinc,nickel and cobalt.After leaching,the gangue is separated from the solution in a thickener,the underflow being discarded.

As the process efficiency is highly influenced by the presence of impurities,a purification step follows.The commonly accepted method of purifying a manganese solution is by the addition of ammonium sulphide to precipitate impurities as insoluble sulphides.The maximum level of some impurities that can be tolerated in the electrolyte solution is given in Table 2 (section 1.2.4)

After this purification section, the ammonium and manganese sulphate solution is fed to the electrowinning cells, where the manganese deposits on the cathodes. The anolyte is recycled to the leaching process. The metal is then stripped from the cathode plates, washed, dried, dehydrogenated and packed. Figure 1 gives a schematic flow diagram of the manganese electrowinning process.

The aim of this project is to formulate a model of the electrodeposition operation in a fundamental way as possible. Where existing theory is not applicable to conditions found in an industrial cell, a semi-empirical approach will be adopted. The resulting model should be capable of predicting the performance of the cells for a given set of input parameters. It should also indicate where improvements can be made in the design, operation and control of this section of the plant.

## 1.2 - The Manganese Electrowinning cell

The cell consists of a number of cathodes and anodes, each pair being separated by a propylene diaphragm, and held together in a set of wooden frames. The manganese metal is then plated on the cathode surfaces, with the simultaneous evolution of hydrogen gas. Impurities, which are present in the catholyte in very small quantities, co-deposit with the manganese on the cathode plate. These impurities generally enhance the evolution of hydrogen, with the result that current efficiencies with respect to the manganese deposition are usually less than 75%. This cathodic current efficiency should be maximized for optimum process performance. The pH is kept as high as possible but below the value at which the precipitation of Manganese hydroxide $Mn(OH)_2$ occurs. The presence of particulate mat[illegible]h as manganese hydroxide and gypsum, block the diaphragm pores.

FIGURE 1 - Simplified Flow Diagram of a Typical Industrial Manganese Production

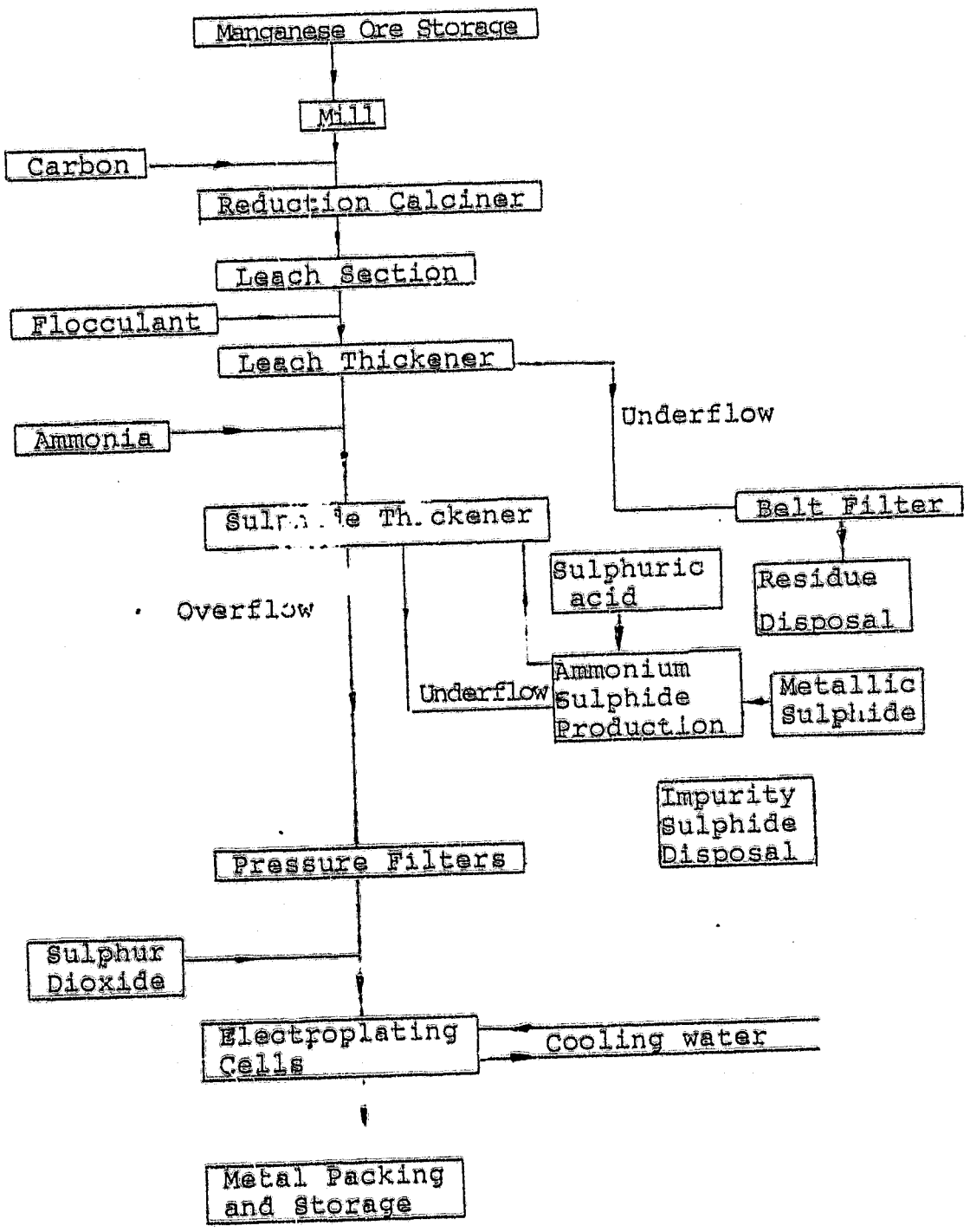

FIGURE 1 - Simplified Flow Diagram of a Typical Industrial Manganese Production

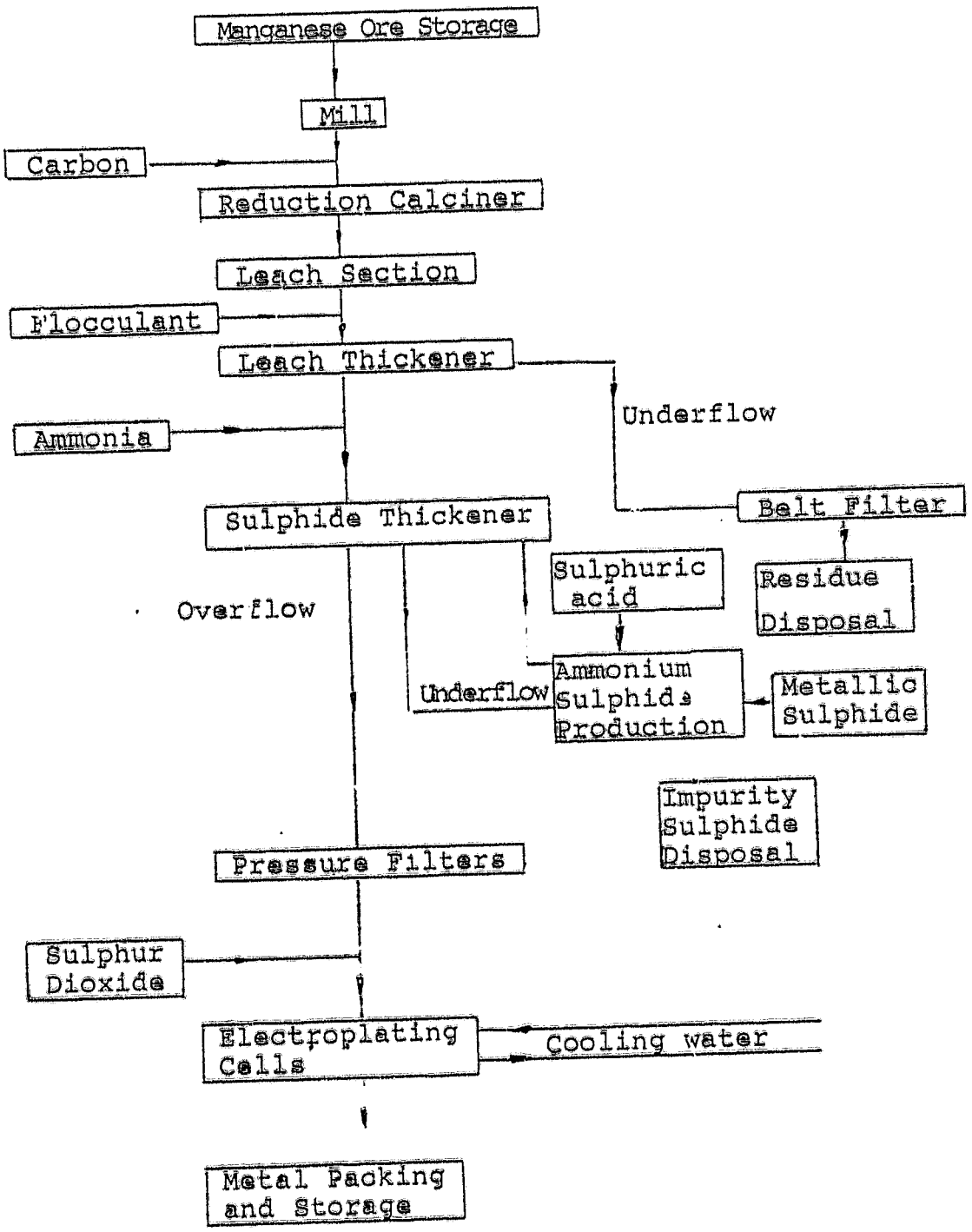

The presence of ammonium sulphate buffers the catholyte solution,allowing the pH to rise to values of the order of 7.8 at the usual operating temperatures without precipitating manganese hydroxide.

The solution then passes through the diaphragm into the anode compartment.Oxygen is evolved and hydrogen ions produced due to the decomposition of water.This forms sulphuric acid ,lowering the anolyte pH to very acidic values.The presence of the diaphragm between the anolyte and catholyte allows these two solutions to have such different compositions.

1.2.1 - Cell Design Considerations

Baggot(4) reports some hystorical background on the subject of cell design.An early type of cell involved each cathode being placed in a separate compartment,as shown in Figure 2 below

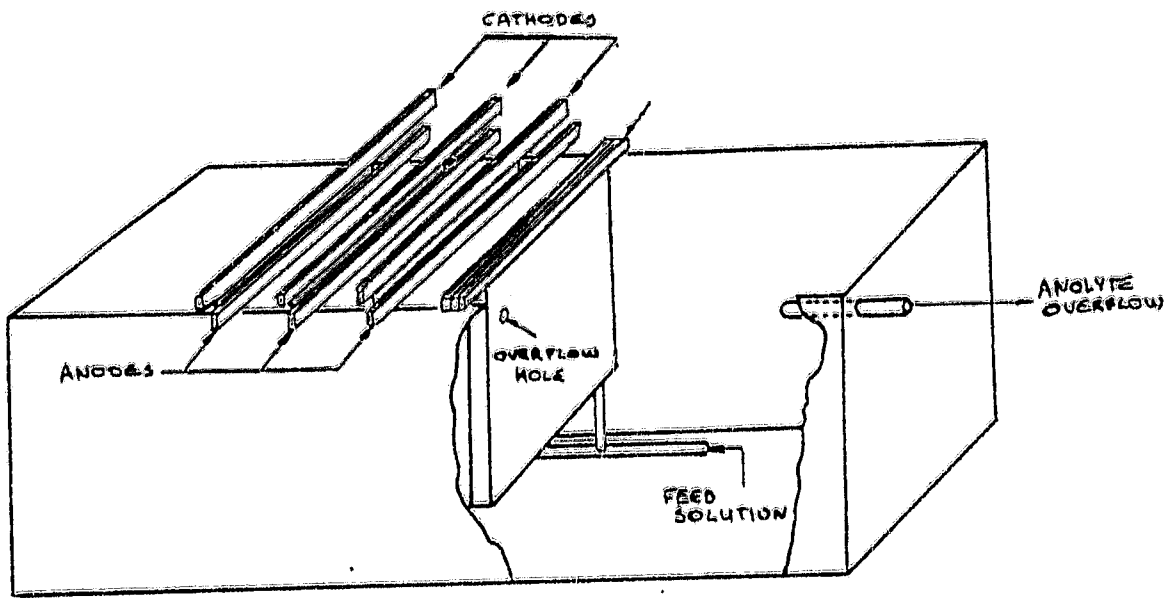


FIGURE 2 - Bottom Feed Cathode Frame Type Cell

This type of cell facilitates the collection and removal of the manganese dioxide deposited at the anode.Each cathode compartment is separately fed whereas all anodes operate in a common anolyte,which constitutes the major part of the cell contents.

Alternately,a cell can be constructed as in Figure 3, in which each anode is located in a frame and bag and anolyte from each frame is separately discharged into a side launder.In this case,all cathodes are immersed in a common catholyte,which forms the bulk of the solution in the cell.The main disadvantage in this case is the removal of anodic manganese dioxide from the individual bags.

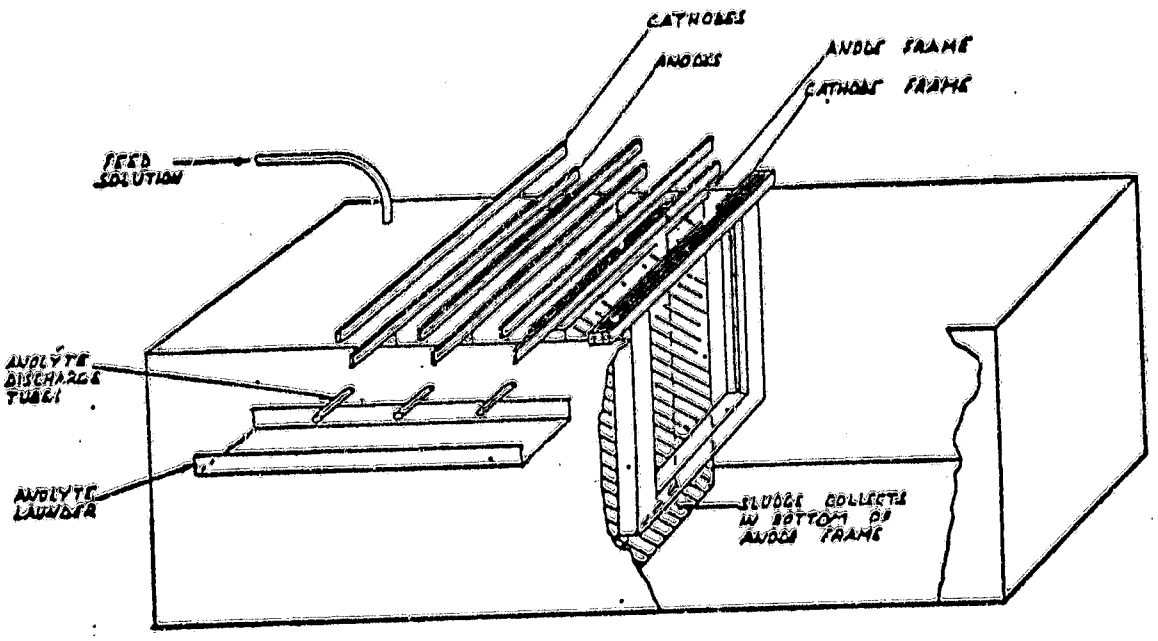


FIGURE 3 - Individual Side Discharge Type Cell

The false bottom cell principle is now the type favoured by most producers.This is the case of the Delta plant,whose operational data was used for the development of this study. A simplified diagram showing the false bottom type cell is shown in Figure 4 below.

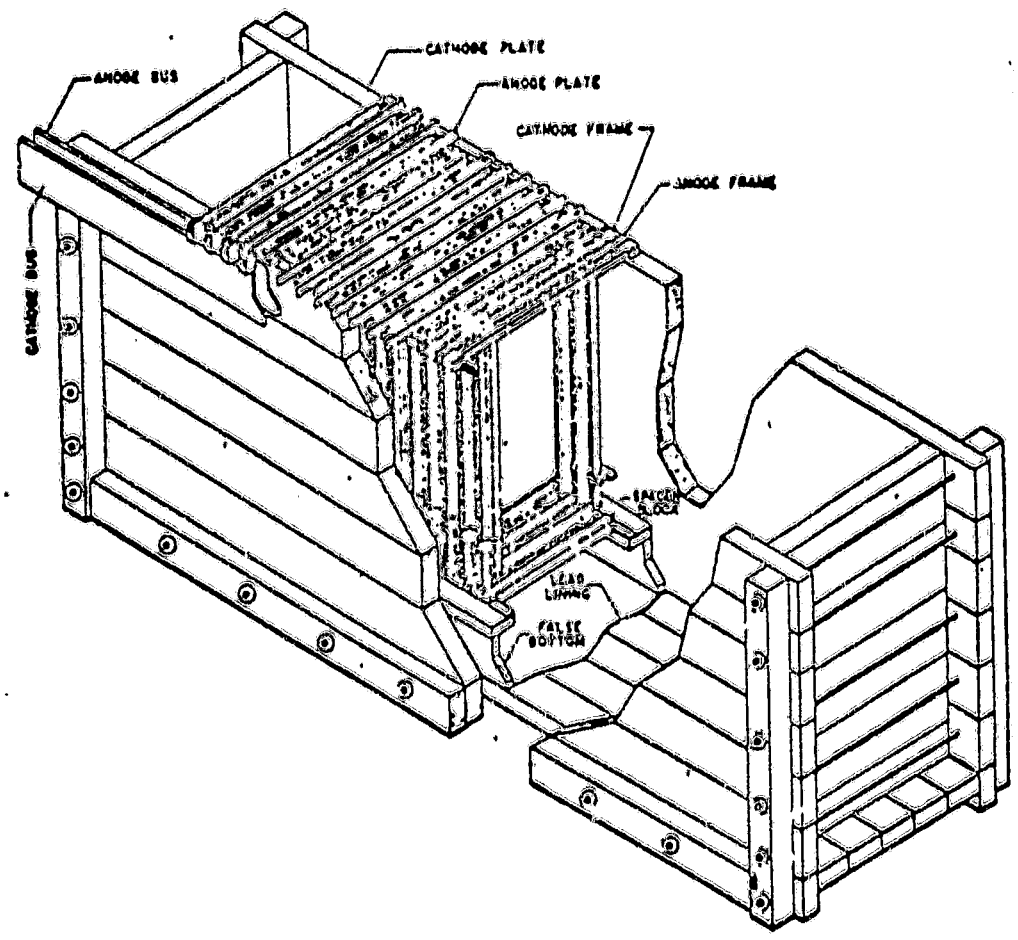


FIGURE 4 -False Bottom Type Cell

At Delta(3),the anodes and cathodes are supported and located in wooden frames.The cathode frame is covered with a diaphragm cloth , which is usually made from propylene.Anode and cathode frames are clamped together on a steel stand,which rests on a shelf in the cell.The cell body is usually constructed from glass fibre reinforced plastic.

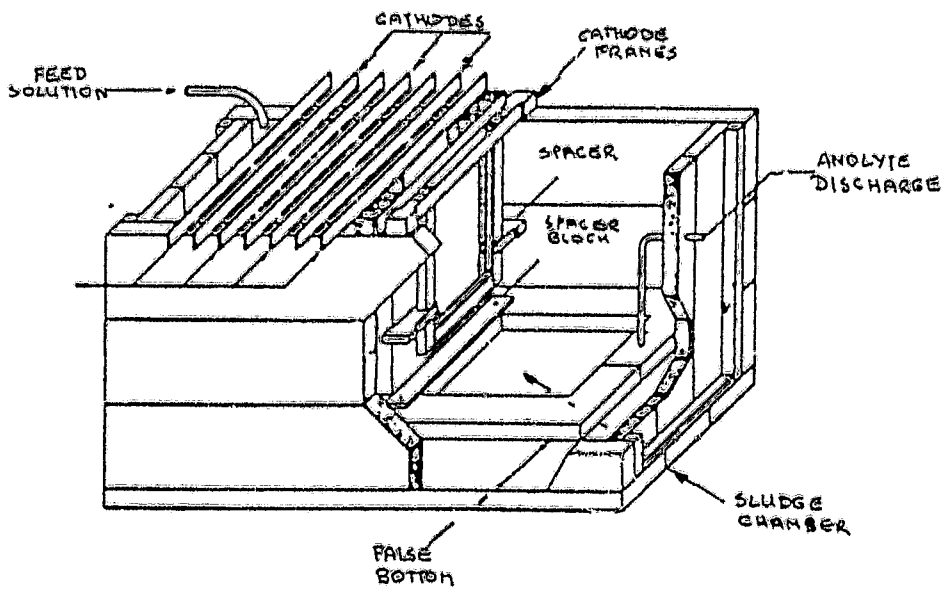


FIGURE 5 - <u>False Bottom Type of Manganese Electrowinning Cell as used at Delta</u>

Feed solution enters a common compartment surrounding the frame where the cathodes and anodes rest,feeding each cathode compartment through slots on the sides of the frame.This produces a rapid circulation(4) in the cathode bag causing less gassing due to hydrogen evolution.The solution (3) flows past the cathode and through the diaph-

ragm into the anode compartment.It leaves the latter through an opening at the bottom into a common anolyte sump,where the manganese dioxide $MnO_2$ formed accumulates,thus not occupying solution space(2).The solution then flows up from this sludge chamber through an adjustable raiser pipe, which controls the solution level in the cells.The anolyte then leaves the cell bank through an overflow weirbox.

The advantages of this type of cell are(4)

- less gassing due to hydrogen evolution , since appreciable coalescence of small bubbles occurs in the catholyte compartment
- a longer cell life,owing to improved removal of manganese dioxide
- simpler cooling,since the cooling coils can be placed on the side of the catholyte compartment and can be replaced while the cell is operating.

Figure 6 below shows a simplified diagram of an elementary cell unit with a cathode plate,surrounded by the diaphragm cloth,and an anode frame.Figure 7 shows ,schematically, the cooling coils next to the cathode compartment.Figure 8 shows a diagramatic sketch of the false-bottom side-feed cathode-frame cell (4),which is similar to that used in Delta.

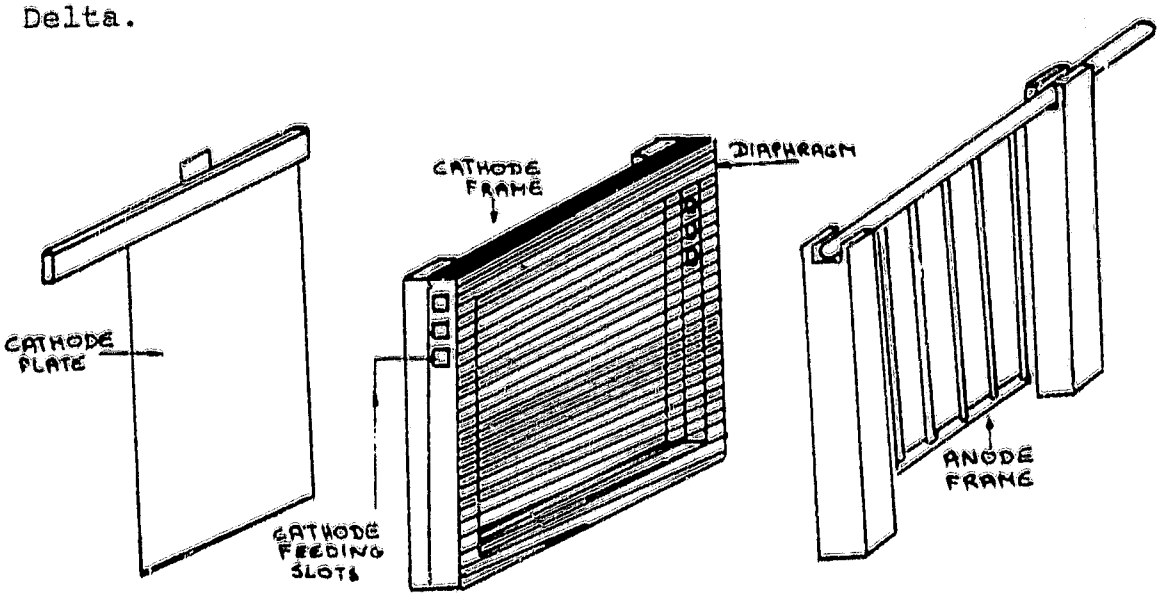


FIGURE 6 -Schematic Diagram of Cathode and Anode Frames with Diaphragm.

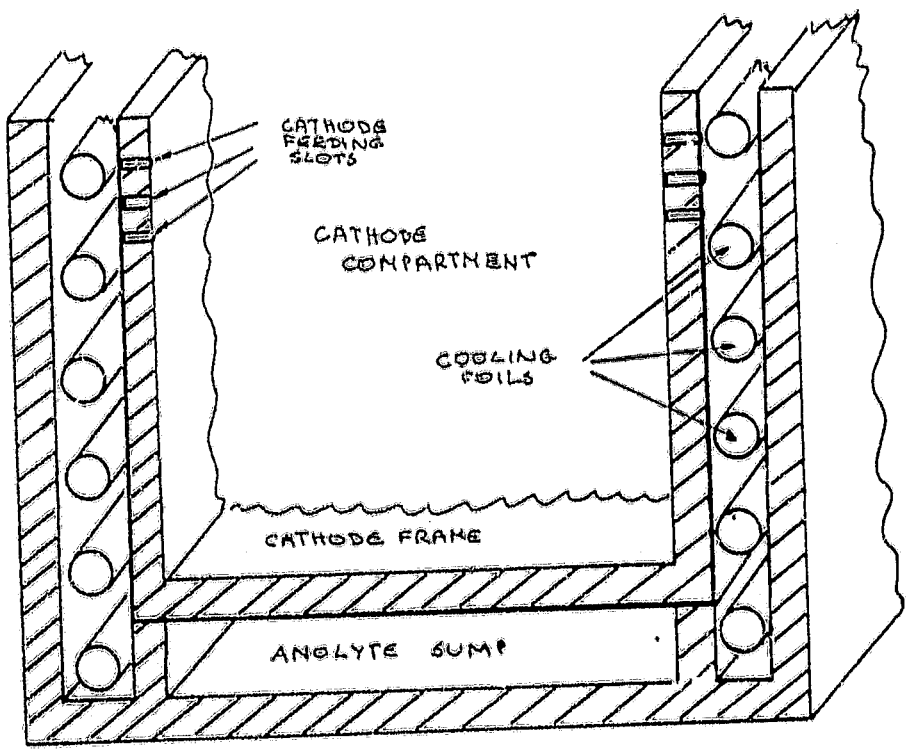


FIGURE 7 - Schematic Diagram of the Cooling Coils on a Cathode Frame

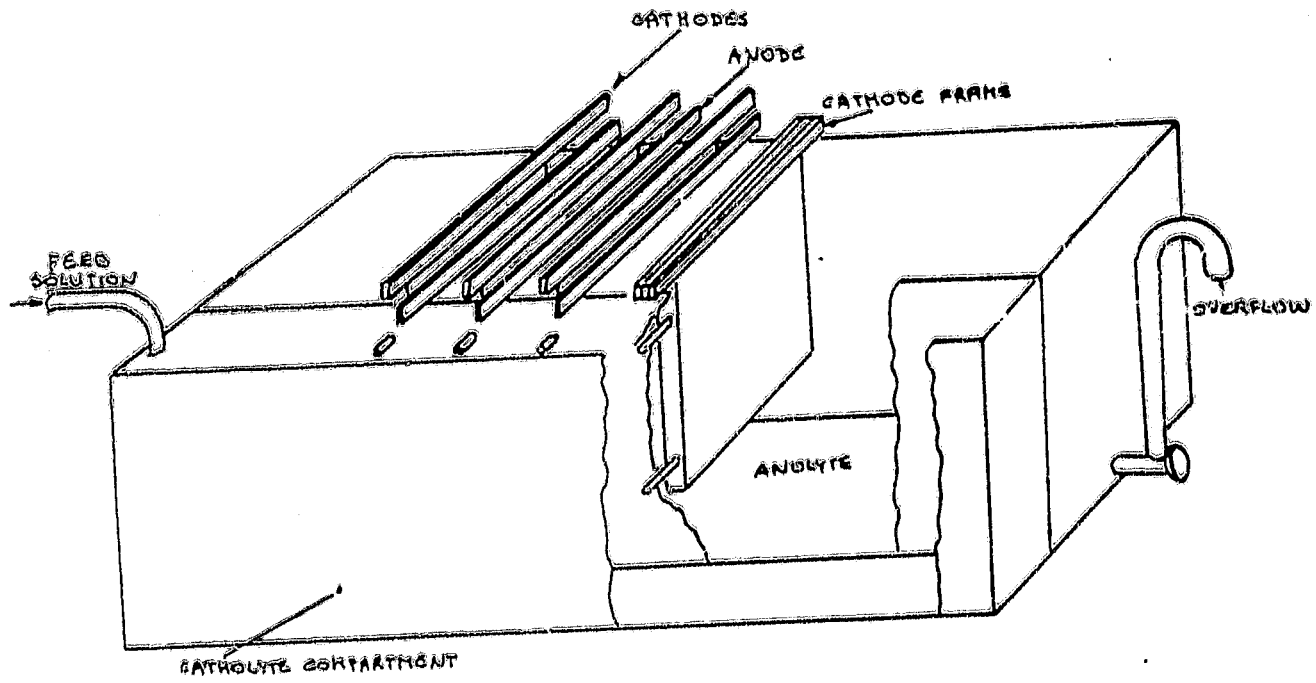


FIGURE 8 - Sketch of the False-Bottom Side-Feed Cathode Frame Manganese Cell

### 1.2.2 - Cathodic Manganese Deposition

Manganese may be formed in either alpha or gamma phase. In commercial scale electrolytic manganese production the metal is deposited in the alpha form in order to have the required characteristics for an industrial operation.According to Dean(2),manganese is first deposited from the solution in the gamma phase.In this modification the process can not be carried out for long enough without the drop of current efficiencies to unacceptable levels.The presence of a sulphur compound performs the role of transforming the initial gamma deposits into finely grained alpha layers allowing acceptable current efficiencies to be maintained over 24 hours.

During the metal deposition a balance must be maintained between the adhesion of metal to the surface,so as not to redissolve,and the easiness of taking the metal off,once the electroplating is ended.The choice of cathode material is vital when considering this balance.

### 1.2.3 - Choice of Electrodes

Experience with industrial production of electroplated metals has shown that certain properties are required for the anodes and cathodes used to obtain optimal operation.

When considering the choice of anode,the following characteristics are important:

(i) insolubility to the solution used
(ii) good electrical conductivity
(iii) acceptable oxygen overvoltage

After years of practice and experimentation with different metals,an alloy made out of 99% lead and 1% silver is the best choice,so far,for the manganese process.Since oxygen

evolution is favoured at high current densities,the anode surface area is made smaller than that of the cathode.The anode shape most commonly used is a set of parallel cylindrical rods of the lead-silver alloy(2),as shown in Figure 6.

As the metal is deposited on the cathode surface,the choice of this electrode is much more involved.The properties required are (3)

(i) insolubility in the cathode
(ii) insolubility in dilute sulphuric acid,which is used for cleaning
(iii) low electrical resistance and good flexibility
(iv) a high hydrogen overvoltage
(v) surface properties which allow the manganese deposited to be easily removed.

The most widely used material is stainless steel ,which is usually treated with sodium silicate,prior to the deposition.This leaves a thin film on the cathode surface that prevents the plated manganese from adhering too tightly to the surface.

### 1.2.4 - Characteristic Operating Conditions

The characteristic feed conditions used in most practical applications are given in Tables 1,2 and 3 -data from reference (3)

TABLE 1 -Characteristic Composition of Cell Feed Solution

| | |
|---|---|
| Manganese as Manganese Sulphate..... | 30-34 kg/m$^3$ |
| Ammonium Sulphate..... | 120-130 kg/m$^3$ |
| Sulphur Dioxide..... | 0.2-0.4 kg/m$^3$ |
| pH value..... | 6.7-7.2 |

TABLE 2 - Maximum Levels of Impurities in Cell Feed Solution

| | ppm |
|---|---|
| Nickel | 1 |
| Cobalt | 0.3 |
| Iron(ferrous) | 15 |
| Silicon | 10 |
| Copper | 5 |
| Zinc | 10 |

TABLE 3 - Typical Analysis of Electrolytic Manganese

| | Low Oxygen Grade % | Low Hydrogen Grade % |
|---|---|---|
| Manganese | 99.82 | 99.65 |
| Sulphur | 0.024 | 0.026 |
| Iron | 0.001 | 0.001 |
| Carbon | 0.006 | 0.006 |
| Oxygen | 0.08 | 0.30 |
| Hydrogen | 0.018 | 0.0006 |

The manganese concentration in the feed is 30-34kg/$m^3$ ,dropping to about 12kg/$m^3$ in the catholyte.The ammonium sulphate,in the range of 120-130 kg/$m^3$ ,effectively acts as a buffer to prevent the precipitation of manganese hydroxide and to increase the conductivity of the electrolyte.Cathodic current densities between 450 and 600 A/$m^2$ are commonly used,being the optimal in the region of 550 A/$m^2$ at an operating temperature of 40°C.

Maximum impurity levels allowed in the feed solution are shown in Table 2.Above these levels their effect on the overall process efficiency would be disastrous as

(i) the current efficiency on the cathode side decreases drastically

(ii) the manganese starts redissoloving in the catholyte

(iii) cracking and peeling of the plated manganese occurs and

(iv) very nodular and brittle deposits are formed , which are very difficult to remove.

The typical analysis of the product metal is shown in Table 3 (3). The manganese is of high purity,showing only traces of Sulphur,Iron and entrained Hydrogen and Oxygen.

## 1.3 - Effects of Parameters on the Manganese Electrodeposition Process

A number of papers in the literature study the effect of individual parameters on the performance of manganese electrodeposition.It is highly likely ,however,that interactions between variables have a significant effect on the process.By attempting to set up a fundamentally based model this dissertation aims at the understanding and prediction of the effect of changing variables simultaneously on the overall performance of the manganese electrowinning cell.

### 1.3.1 - Manganese Sulphate Concentration

The accepted manganese sulphate concentration in the catholyte for optimum deposition is around 12 kg/m³ as Manganese(3),(5).Feed solution concentrations between 30 and 40 kg/m³ Mn have been reported by Dean(2), Woodman(5) and Martin(6).It is desirable to keep the outflowing manganese concentration as low as possible. The lower this concentration,the lower the amount of manganese returned to the leaching solution,hence reducing flow rates and required sizes of equipment.The manganese concentration in the catholyte should,however,not be allowed to drop too low ,as insufficient manganese ions at the cathode surface would result in redissolution of the plated manganese.As the concentration of manganese in the catholyte goes above the desired limits,the ease to remove the deposited metal from the cathode surfaces is affected.A high manganese content also results in excessive treeing of the deposit.If very high,manganese hydroxide $Mn(OH)_2$ will precipitate from the solution. The solution pH and manganese concentration are interrelated.The higher the manganese concentration,the lower is the maximum pH that can be tolerated to avoid precipitation of manganese hydroxide.

### 1.3.2 - Ammonium Sulphate Concentration

Dean(2) and Jacobs(5),(7) and (8),report an optimum ammonium sulphate concentration in the catholyte of 135 to 140 kg/m³.This compound plays an important role in the electrodeposition process as it increases the solution conductivity and buffers the catholyte between pH 7 and 8 ,so that the precipitation of $Mn(OH)_2$ can be avoided. Manganese hydroxide is very detrimental to the performance of the electrolytic cell as it blocks the diaphragm and also tends to adhere to the cathode deposit.

Various theories have been proposed to explain the buffering effect of ammonium sulphate on the manganese solution.Tilak et al (9) suggest that it is caused by the formation of a manganese-ammonia complex,which lowers the concentration of the manganese cation ($Mn^{2+}$) in the solution.This increases the solubility of manganese in the solution as the element is now distributed between $Mn^{2+}$ and the manganese-ammonia complex,allowing higher pH's to be reached without precipitation of the manganese hydroxide.This increase of electrolyte pH is beneficial to the current efficiency on the cathode side.The observations of Dean(2) seem to agree with Tilak et al (9), as he states that ,beyond the pH control,the ammonium ion appears to increase the difficulty with which the hydrogen ions are discharged.

Kublanovskii et al (10) report the formation of various manganese sulphate complexes ,as an alternative solution to the buffering effect of the ammonium sulphate.The predominant compound would be $MnSO_4$

The available experimental evidence suggests however that the formation of the ammonia-manganese complex is more important in determining the properties of the catholyte.

### 1.3.3 - The Addition of Sulphur Compounds

It is now generally accepted that in the commercial process for manganese deposition ,the metal is initially deposited in the gamma form,but current efficiencies can only be maintained in those cases where,after the deposition of a few microns of metal,the gamma form undergoes a transformation(4),(11).After this initial transformation to alpha-manganese ,subsequent deposition will occur in the alpha form.Fortunately this transformation can take place at room temperature and is accelerated by the presence of

sulphur compounds,particularly sulphur dioxide ($SO_2$). A concentration of 0.1kg/m³ of sulphur dioxide,(2) (5), in the solution gives the plated metal optimum adhesion to the cathode surface.

Tilak et al (11) studied the kinetics of the electrodeposition process using sulphur dioxide in solution.They concluded that the presence of the sulphur dioxide lowers the cathodic current efficiency.However as the compound's concentration increases,in the solution, so does the current efficiency.They also found that below certain current densities the deposited metal redissolves.The addition of small quantities of sulphur dioxide increases this limiting current density below which redissolution of the metal occurs.But if large quantities are added, this limiting current density is lowered.Thus there is an optimum amount of sulphur dioxide which should be kept in solution for best overall process performance,this being of the order of 0.1kg/m³.

### 1.3.4 - Solution Temperature

Typical operating temperatures for optimum process performance are around 40°C.As the electrodeposition reaction of manganese metal from the ion in solution is exothermic, energy must be removed in order to keep the solution temperature at the optimum.This is done by having cooling water coils immersed in the electrolyte.

Dean(2) and Jacobs(7) report an optimum operating temperature of 35°C at a current density of 400A/m², which is supported by Shulyakas et all (12).Louis and Martin(6) made more recent investigations on the effect of this parameter on current efficiency ,and reported a value of 40°c at a current density of 400A/m².

### 1.3.5 - Current density

Current density is one of the most important parameters to be considered on an industrial scale electrodeposition process for economic reasons.It is directly related to the power consumption of the plant.The parameter 'power consumed per unit mass of manganese' is minimized for optimum overall plant performance.

When all the other plant parameters are kept constant under controlled conditions,the current efficiency shows a maximum when plotted against current density.Various authors report this ,although they differ slightly on the absolute value of this maximum.Dean(2) reports a value of 480A/m² at 35°C,whereas Louis and Martin(6) report 550 A/m² at 40°C.

### 1.3.6 - Solution pH

Catholyte pH is related to most of the other operating variables and can not be controlled independently.It is particularly sensitive to feed solution purity and flow rate.The reported trend by most of the cited authors is that the higher the pH the higher the current efficiency on the cathode side.This is demonstrated by a quantitative study made by Louis and Martin(6).However it is not possible to increase the pH indefinetely due to the eventual precipitation of manganese hydroxide.

1.3.7 - Impurities in the Catholyte

The impurities that are present in the catholyte are completely dependent on the manganese ore which is used and also on the performance of upstream equipment.Depending on the impurities'nature they have either detrimental or beneficial effects on the deposition process.

Commonly reported detrimental effects are the drastic drop of current efficiency due to the presence of small amounts of impurities,and the redissolution of the plated manganese.It was found that the addition of sulphur dioxide in small quantities allows the presence of impurities at higher levels without redissolution taking place(11).The most common detrimental impurities are Cobalt,Nickel,Zinc and Iron.Their simultaneous effect is more drastic than the addition of their individual effects(2),with Nickel and Cobalt being the most harmful impurities.

Beneficial impurities have been reported(6),and their presence in solution improves tne cathodic current efficiency.The two known examples are Selenium and Telurium. However these two are very rare elements and their addition would be very expensive,unless they are present in the ore from which the manganese is extracted.

## 1.4 - The Modelling Exercise

The modelling of electrochemical systems ,as with many other systems,can be carried out in two ways,i.e. statistically and mechanistically.The statistical approach is based on data obtained from operating plants and previous experimental work.This data is then fitted to empirical equations with adjustable parameters.On the other hand, the mechanistic approach is based on existing fundamental knowledge of physical,chemical and electrical changes taking place(13).Both approaches have their advantages and disadvantages.The main disadvantage of the statistical approach is that of extrapolation.The equations are fitted over a narrow region where data is available , and projecting out of this range invariably leads to errors. One of the main advantages is its simplicity,particularly when theory is not well developed.

The mechanistic approach,being based on physico-chemical principles,has the advantage of being able to be extrapolated outside the range of existing experimental evidence. It often happens that equations are complicated and simplifications are required so that the model can be solved mathematically.Often,due to lack of physical and chemical data,further assumptions and the incorporation of adjustable parameters have to be resorted to.

### 1.4.1 - The Statistical Approach

In the present modelling exercise,one section required the partial use of the statistical approach.The kinetics of the deposition processes on the cathode are only partially understood.In addition ,the lack of physical and chemical data,and the difficult task of including

the impurities in the model led to the use of a semi-empirical equation.A study (6) of the effects of current density and temperature on current efficiency provided the required data. The impurity effect was modelled from data obtained from an operating electrolytic manganese plant.The final kinetic model incorporates the simultaneous effect of temperature,current density and impurity level on cathodic current efficiency.

### 1.4.2 - The Mechanistic Approach

Bryson(14) has recently presented a lecture where the modelling exercise of an electrowinning cell in general was analysed.In general outline ,this model follows Bryson's approach.This model includes the mass balance,energy balance transport of ions through the diaphragm,voltage drop model and other minor aspects.Simplifications were made to allow mathematical solution of the equations,and in certain cases, a few variables had to be fitted so that the model would agree with plant data.

# 2. MODEL COMPONENTS

## 2.1 - Logistic of the Model

The model is organized in the form of a logic diagram as shown in Figure 9.The properties of the feed solution are largely dependant on the performance of the plant upstream the cell house,but some control can be usually exrecised on the feed flow rate.The cooling water temperature and flow rate can also be adjusted within certain limits.

Initial estimates are required before the mass and energy balances can be performed,as indicated in Figure 9.These are:

- cathodic and anodic current efficiencies
- cell voltage
- water and ammonia losses
- temperature of anolyte and catholyte

From the feed composition and temperature,the feed ion concentrations of the various aqueous species are determined,using the feed equilibrium relationships and electrical neutrality equation.Knowing this a mass balance is performed,determining the anolyte composition.With this and the solution equilibrium conditions ,the anolyte ion concentrations are determined.An energy balance is then performed to calculate the anolyte and catholyte temperatures. All the calculated values are then compared to the initial estimates,and if agreement within certain limits is achieved, the calculation proceeds to the next section.

The diaphragm model that follows determines the catholyte composition.Once this is known,individual aqueous species concentrations are calculated from equilibrium conditions and electrical neutrality equation.On completion of these,

FIGURE 9 - Logic Diagram

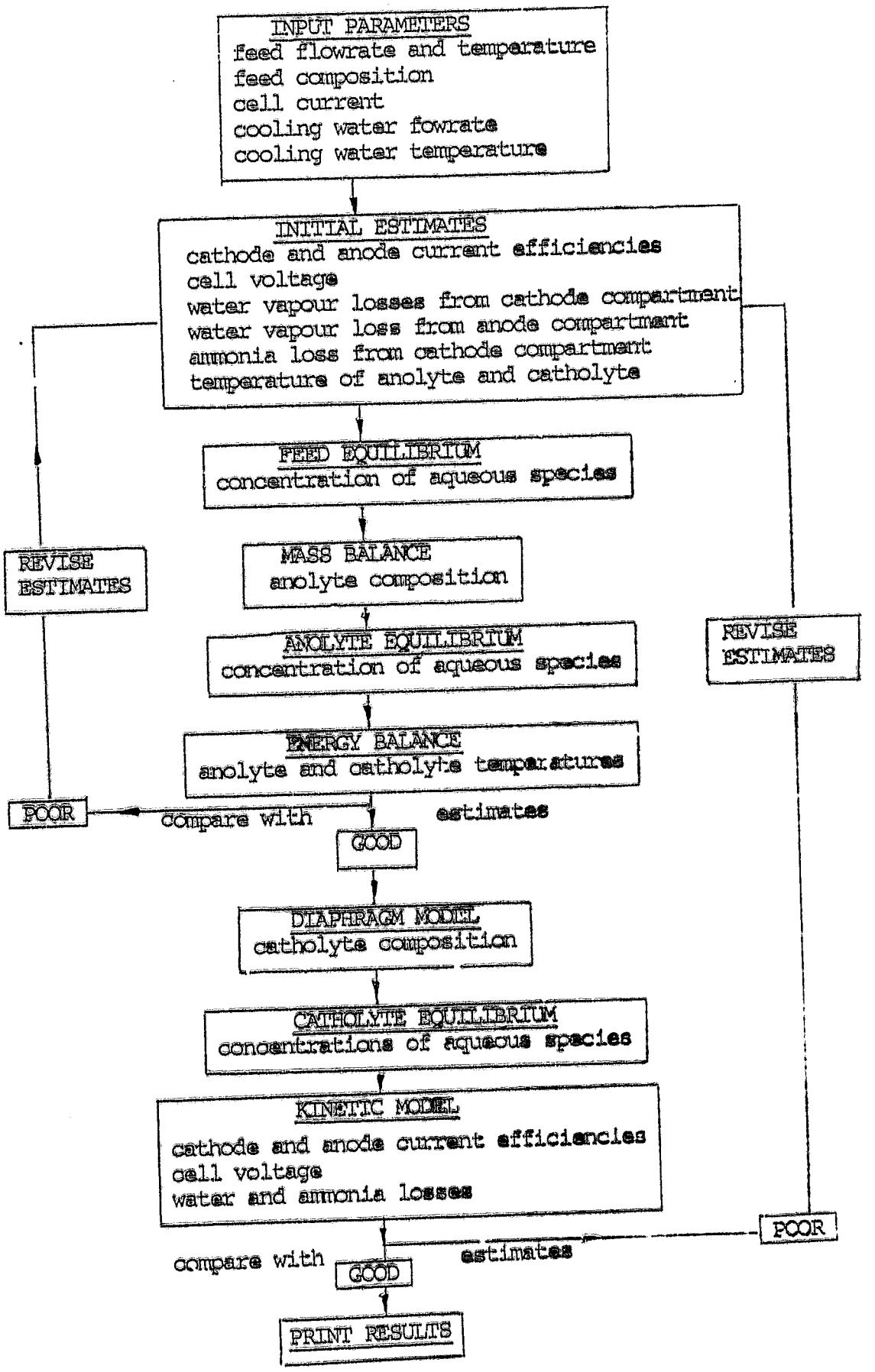

the kinetic model is performed,and the cathodic and anodic current efficiencies are found.The cell voltage model is also used ,as well as the calculation of water and ammonia losses.The values determined through this procedure are the compared again with the initial estimates. Adjustments are made where necessary and the whole procedure is repeated until satisfactory agreement is achieved.

The various model components are now presented.

## 2.2 - Solution Equilibria

A manganese sulphate - ammonium sulphate solution has different aqueous species depending on its pH.In the pH range of 6.0 to 8.0 it contains $H_2O$ , $Mn^{2+}$ , $NH_4^+$, $MnNH_3^{2+}$ , $NH_3$ and $SO_4^{2-}$ , whereas at a pH less than unity $H_2O$ , $Mn^{2+}$ , $H^+$ , $NH_4^+$ , $SO_4^{2-}$ and $HSO_4^-$ occur in significant quantities. To determine the concentrations of the various components from equilibrium constants K,it is necessary to know activity coefficients for all the species present.As very little data is available for concentrated solution mixtures,equilibrium ratios K' have been measured or estimated over the range of variables applicable in this study.These equilibrium ratios K', are the direct relationships among the various concentrations of the species present in solution.

The experimental determination of pH causes problems as currently available methods merely produce a number on a scale which is fixed by a set of standard buffer solutions. In concentrated mixtures of ions and neutral species, the experimentally measured pH values are therefore not necessarily related directly to the concentration or activity of the hydrogen ion, as reported by Bates(15).In this dissertation we will ,for convenience, define an

effective hydrogen ion concentration in the catholyte as

$$-\log_{10} Y_2 = \text{measured pH value}$$

Similar definitions will be applied for the feed and anolyte solutions.

The nomenclature for the different ionic and neutral species present in the electrolyte solutions is tabulated below (Table 4).

TABLE 4 - Nomenclature for Aqueous Species

| Component | Concentrations (kmole/m³) | | |
|---|---|---|---|
| | Feed | Catholyte | Anolyte |
| Total Mn | $X_m$ | $Y_m$ | $Z_m$ |
| Total $NH_3$ | $X_a$ | $Y_a$ | $Z_a$ |
| $Mn^{2+}$(aq) | $X_1$ | $Y_1$ | $Z_1$ |
| $H^+$ (aq) | $X_2$ | $Y_2$ | $Z_2$ |
| $NH_4^+$(aq) | $X_3$ | $Y_3$ | $Z_3$ |
| $MnNH_3^{2+}$ (aq) | $X_4$ | $Y_4$ | - |
| $NH_3$(aq) | $X_5$ | $Y_5$ | - |
| $SO_4$ (aq) | $X_6$ | $Y_6$ | $Z_6$ |
| $HSO_4^-$ (aq) | - | - | $Z_7$ |
| $Ni^{2+} + Zn^{2+} + Co^{2+} + Fe^{3+}$ (aq) | - | $Y_8$ | - |

2.2.1 - Feed and Catholyte Equilibrium

Ammonium sulphate is added to the electrolyte because it acts as a buffer to the solution in the pH range of 7 to 8 through the formation of the manganese - ammonia complex.

$$Mn^{2+} + NH_4^+ \rightleftharpoons MnNH_3^{2+} + H^+ \qquad (2.1)$$

The equilibrium of this reaction has been studied by Tilak et all (11),indicating a weak complex.Bryson(unpublished data)has studied experimentally, the equilibrium ratio of this reaction ,and his values are shown in Appendix D.1 . These were modelled using a linear fitting on a logarithmic scale and the following expression was found to hold reasonably well for the temperature range of $295 < T < 330$

$$K_c' = \frac{Y_2\ Y_4}{Y_1\ Y_3} = \exp(-34.57 + 0.051T) \qquad (2.2)$$

A second effect of adding the ammonium sulphate is to increase the electrical conductivity of the electrolytic solution.This is advantageous as the cell voltage will be lower and will thus require less power for a given current density.

The neutral $NH_3$ species is also present in significant quantities.The ammonium ion - ammonia equilibrium is

$$NH_3 + H^+ \rightleftharpoons NH_4^+ \qquad (2.3)$$

The equilibrium ratio for this reaction has been extensively studied,and the data is given by Weast(16) has been modelled and adapted for usage in the study(please refer to Appendix D.2).In the temperature range

$295 < T < 330$ the data is adequately represented by the equation

$$K'_a = \frac{Y_3}{Y_2\ Y_5} = \exp\ (40.32 - 0.064\ T\ ) \qquad (2.4)$$

The hydrogen gas which evolves at the cathode strips part of the neutral ammonia species present in the catholyte, resulting in significant $NH_3$ losses. This loss is modelled proportionally to the concentration of neutral $NH_3$ in the liquid phase, as presented in section 2.6 .

A further problem which could arise in the catholyte is the precipitation of manganese hydroxide $Mn(OH)_2$ . This will occur if the solubility limit for $Mn(OH)_2$ is exceeded. The reaction responsible for the precipitation is

$$Mn^{2+} + 2\ H_2O \rightleftharpoons Mn(OH)_2(s) + 2\ H^+ \qquad (2.5)$$

The equilibrium ratio for this reaction has been studied by Bryson (unpublished data) and is modelled in Appendix D.3 by

$$K'_s = \frac{Y_2^{\,2}}{Y_1} = \exp\ (-65.17 + 0.1025\ T\ ) \qquad (2.6)$$

in the temperature range $295 < T < 330$ . By letting

$$\triangle Y_1 = \frac{Y_2^{\,2}}{K'_s} - Y_1 \qquad (2.7)$$

then precipitation of manganese hydroxide will occur if $\triangle Y_1 < 0$ .

The formation of this precipitate is catastrophic to the efficient operation of the manganese electrodeposition process. It blinds the pores of the diaphragm and it tends to deposit in patches on the manganese metal causing copious hydrogen evolution on those areas.

## 2.2.2 · Anolyte Equilibrium

As the anolyte pH is very low, in the region of unity, some of the species present in the feed and catholyte solutions have neglegible concentrations in the anolyte. These are the manganese-ammonia complex $MnNH_3^{2+}$, and free ammonia $NH_3$. However the formation of the bisulphate ion $HSO_4^-$ largely determines the hydrogen ion concentration in the anolyte, the reaction being as follows

$$HSO_4^- \rightleftharpoons H^+ + SO_4^{2-} \qquad .(2.8)$$

Young et al (17) have proposed a correction factor that can be applied to the equilibrium constant to determine the equilibrium concentration ratio. This factor is given as a function of total ionic strength, but it does not include temperature as a variable. Comparing operating conditions in a typical manganese electrowinning plant with those described by the above procedure, an inedequate correlation is found between them. The following expression, however, fits the available data to a reasonable degree of accuracy

$$K_h' = \frac{Z_2\ Z_6}{Z_7} = \exp(8.339 - 0.0294\ T) \qquad (2.9)$$

The details of the modelling exercise on this equilibrium ratio are presented in Appendix D.4

## 2.3 - Diaphragm Model

The operating conditions of a manganese electrowinning cell are such that the diaphragm allows the two electrolytes to have very different properties.It is important to be able to model the flux of the ionic species through the diaphragm.Bryson and Lawrence(18) have developed a flux equation for transport in a diaphragm of a chlor-alkali cell.As very little information is available for manganese cells,the interaction diffusion coefficient , incorporated in their model,will be assumed to be zero. The various diffusion coefficients are determined using data from the operating manganese plant at Delta.

The mass flowrate of the jth species through the diaphragm at a distance x from the cathode side can be expressed as

$$W_j = Q_o\, B_j(x) - \frac{I\, F\, D_j\, z_j\, B_j(x)}{R\, T\, k^*} - \varepsilon\, A\, D_j \frac{dB_j(x)}{dx} \qquad (2.10)$$

where $k^*$ is the average conductivity of the solution,i.e.

$$k^* = \frac{F^2}{R\, T} \Sigma \left[ z_j^{\,2}\, D_j\, (Y_j + Z_j) \,/\, 2 \right] \qquad (2.11)$$

A more detailed development is presented in Appendix E.

The boundary conditions applying to the equation (2.10) are

$$B_j(0) = Y_j \quad \text{and} \quad B_j(d) = Z_j \qquad (2.12)$$

Integrating (2.10) yields

$$W_j = \frac{\alpha_j D_j \left[ Z_j - Y_j \exp\left(-\frac{\alpha_j d}{\varepsilon A}\right) \right]}{1 - \exp\left(-\frac{\alpha_j d}{\varepsilon A}\right)} \qquad (2.13)$$

where

$$\alpha_j = \frac{I F z_j}{R T k^*} - \frac{Q_0}{D_j} \qquad (2.14)$$

The polypropylene diaphragm used in electrolytic manganese cells has the following properties

$d = 1.37 \quad 10^{-3}$ m
$\varepsilon = 0.67$
$A = 100.8$ m$^2$

It is found that only the transport of $H^+$ and $NH_4^+$ species need be considered due to the following reasons

(1) the manganese concentrations in both the catholyte and anolyte are very similar

(2) $MnNH_3^{2+}$ and $NH_3$ react rapidly with hydrogen ions $H^+$ migrating through the diaphragm, and it is assumed here that this occurs effectively at x=0 (i.e. the catholyte side of the diaphragm)

(3) the bisulphate ion $HSO_4^-$ also dissociates rapidly as soon as the pH increases, and its concentration is assumed to be effectively zero at x=d (i.e. the anolyte surface of the diaphragm)

(4) the transport of $SO_4^{2-}$ is obtained from the electrical neutrality equations.

Using the data from the Delta plant ,the diffusion coefficients for the hydrogen and ammonium ions were evaluated and the following average values obtained

$$D_2 = 8,23 \times 10^{-9} \ m^2/s$$

$$D_3 = 6,10 \times 10^{-10} \ m^2/s$$

These values are assumed constant in the model over the range of the operating conditions studied.

## 2.4 - Kinetic Model

### 2.4.1 - Cathodic Kinetic Model

The following reactions will be assumed to occur on the cathode,with the corresponding partial current densities written on the right of the reactions

$$Mn^{2+}(aq) + 2\ e^- \longrightarrow Mn(s) \qquad (i_1) \qquad (2.15)$$

$$2H_2O + Mn(s) + 2\ e^- \longrightarrow H_2(g) + 2OH^-(aq) \qquad (i_2) \qquad (2.16)$$

$$M^{2+}(aq) + 2\ e^- \longrightarrow M(s) \qquad (i_3) \qquad (2.17)$$

$$2H_2O + M(s) + 2\ e^- \longrightarrow H_2(g) + 2OH^-(aq) \qquad (i_4) \qquad (2.18)$$

M represents divalent metal ions,such as $Co^{2+}$, $Ni^{2+}$ ,$Fe^{2+}$ and $Zn^{2+}$ which codeposit with the manganese.

Let $\varphi$ be the fraction of the plated surface which contains M,the impurity metals.Then

$$\varphi = \frac{i_3}{i_1 + i_3} \simeq \frac{i_3}{i_1} \qquad (2.19)$$

as $i_3 \ll i_1$ (2.20)

The total current density on the cathodic side is made up of all the above partial current densities, i.e.

$$i_c = i_1 + (1 - \varphi)\, i_2 + i_3 + i_4$$

$$\simeq i_1 + i_2 + (i_4 - i_2)\,\frac{i_3}{i_1} \qquad (2.21)$$

Here the assumption (2.20) was used again. Now, defining the fractional current efficiency for manganese deposition as

$$\xi_c = \frac{i_1}{i_c}$$

which, after substituting $i_c$ from equation (2.21) and simplifying becomes

$$\xi_c = \frac{1}{1 + \frac{i_2}{i_1}\left[1 + \left(\frac{i_4 - i_2}{i_2}\right)\right]\frac{i_3}{i_1}} \qquad (2.22)$$

Assuming that all the electrode reactions are first order in concentration, then

$$i_1 = \lambda_1 Y_1 \qquad (2.23)$$

$$i_2 = \lambda_2 Y_2 \qquad (2.24)$$

$$i_3 = \lambda_3 Y_8 \qquad (2.25)$$

$$i_4 = \lambda_4 Y_2 \qquad (2.26)$$

Substituting all the first order kinetic equations in the expression for the fractional current efficiency results in

$$\varepsilon_c = \frac{1}{1 + \frac{\lambda_2}{\lambda_1}\left[1 + (\frac{\lambda_4 - \lambda_2}{\lambda_2})\frac{\lambda_3}{\lambda_1}\frac{Y_8}{Y_1}\right]\frac{Y_2}{Y_1}} \qquad (2.27)$$

The rate of each of the two main reactions , the manganese deposition and its respective hydrogen evolution,may be modelled by Tafel kinetics with linear concentration dependance(i.e. equtions 2.23 and 2.24 ) and series mass transfer resistance,as follows (14)

$$\frac{\lambda_2}{\lambda_1} = \frac{(2\ F\ K_1 + h_1)\ K_2\ h_2}{2\ (F\ K_2 + h_2)\ K_1\ h_1} \qquad (2.28)$$

where

$$h_1 = i_{01}^* \exp\left[\frac{\beta_1 \eta_1\ F}{R\ T}\ (E_{01}^* - E_c)\right] \qquad (2.29)$$

and

$$h_2 = i_{02}^* \exp\left[\frac{\beta_2\ \eta_2\ F}{R\ T}\ (E_{02}^* - E_c)\right] \qquad (2.30)$$

The ratio $\lambda_2/\lambda_1$ is related to the total current density on the cathode side ($i_c$) through equation (2.21).However the last term in this equation is neglegible compared to the other two and can thus be omitted, i.e.

$$i_c \simeq i_1 + i_2 \qquad (2.31)$$

Using this equation,Ec can be eliminated ,but the form of the resulting equation is highly complicated,involving a

large numbers of unknown parameters.

By expressing $\lambda_2/\lambda_1$ as a Taylor series about a current density of 550 A/m² and including the temperature in the exponential form, the MINTEK data (6) was fitted and the following expression was obtained

$$\frac{\lambda_2}{\lambda_1} = \gamma \left[1 + \exp\left(\frac{12300}{T} - 40{,}953\right)\right] \cdot \left[1 - 0{,}0001213 \times (i_c - 550) + 0{,}00001278 \times (i_c - 550)^2\right] \qquad (2.32)$$

It was found that the MINTEK results (6) were consistently lower than those observed on the Delta plant. This is not surprising as the MINTEK results were obtained using a small batch electrowinning cell without a diaphragm and only for a short period of 30 minutes. The form of the equation variation was kept, but the value of $\gamma$ was adjusted to be consistent with plant performance results. For this simulation the value of $\gamma$ used was

$$\gamma = 1{,}36 \times 10^6 \qquad (2.33)$$

Appendix F shows a detailed fitting of the kinetic model. Figures 10 and 11 below, show the MINTEK data (6) and the results of equation (2.32) simulating plant behaviour.

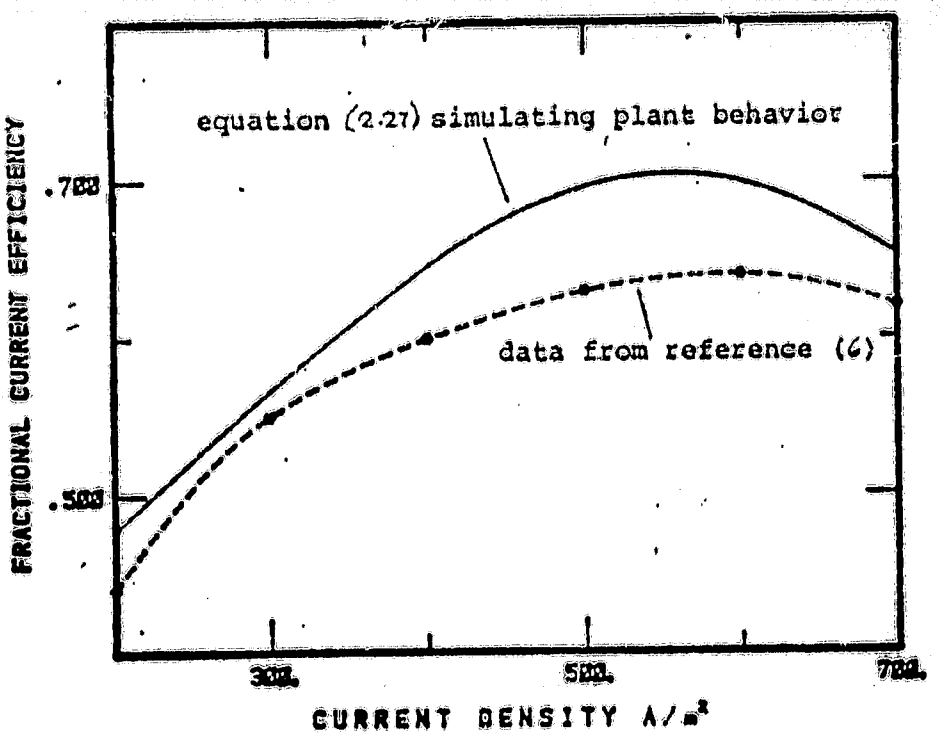


Figure 10 - Effect of Cathodic Current Density
T = 313K; pH = 7.6; $Y_m$ = 0.204 k mol/$m^3$;
$Y_a$ = 1.818 k mol/$m^3$; $Y_\beta$ = 2.6 x $10^{-5}$ k mol/$m^3$.

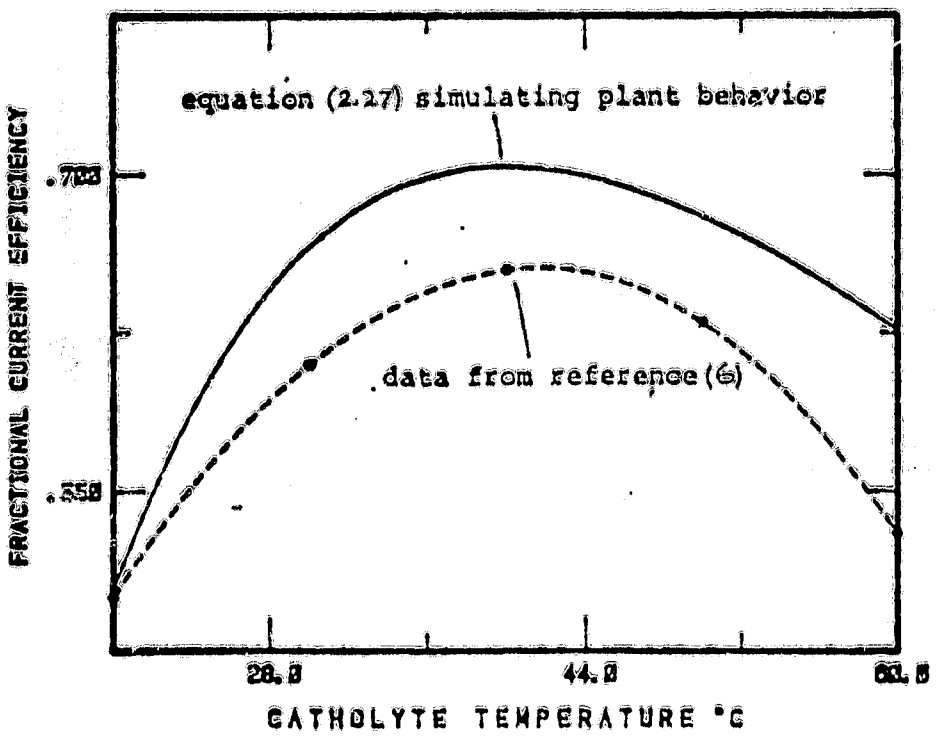


Figure 11 - Effect of Catholyte Temperature
$i_c$ = 550 A/$m^2$; pH = 7.6; $Y_m$ = 0.204 k mol/$m^3$
$Y_a$ = 1.818 k mol/$m^3$; $Y_\beta$ = 2.6 x $10^{-5}$ k mol/$m^3$.

The impurity concentration $Y_8$ is taken as the sum of the nickel,cobalt, zinc and iron content of the catholyte in kmole/m³.An individual effectfor each impurity was not possible to determine as the data available was not sufficient.Although the data available from Delta is fairly scattered,the trend shown by equation (2.27) adequately models the observed behaviour with

$$\left(\frac{\lambda_4 - \lambda_2}{\lambda_2}\right)\frac{\lambda_3}{\lambda_1} = 1850 \qquad (2.34)$$

Figure 12 below shows the results of equation (2.27),with the above figure of (2.34),with the average molecular weight of the impurities as 60 kg/kmole .The details of the impurity model fitting are given in Appendix F

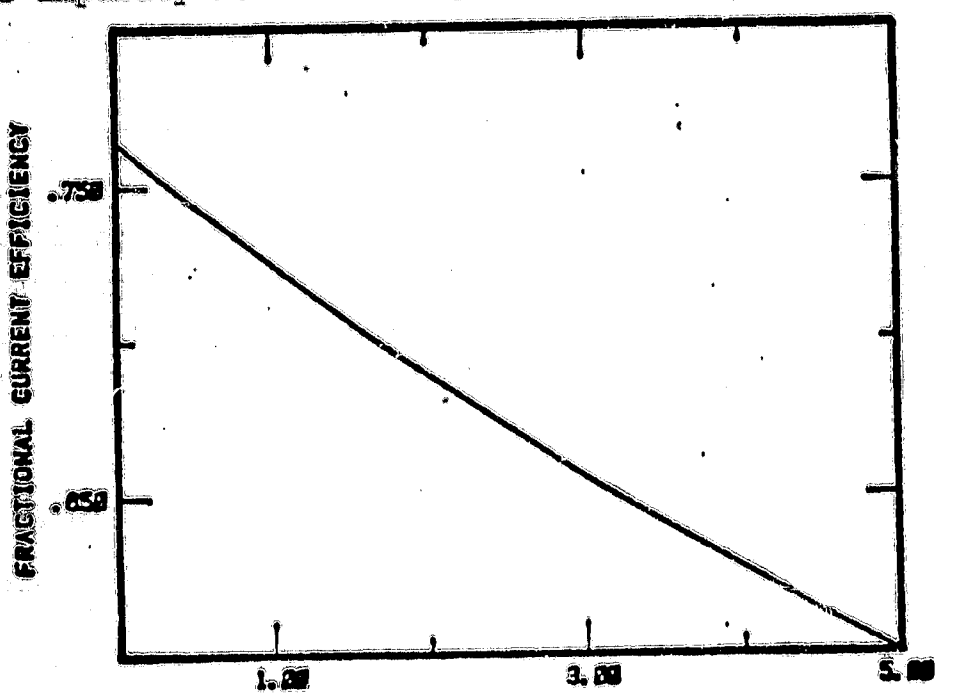


Figure 12- Effect of Impurity Concentration

$i_c$ = 550 A/m²; pH = 7.6; T = 313K

$Y_m$ = 0.204 k mol/m³; $Y_a$ = 1.818 k mol/m³

2.4.2 - Anodic Kinetic Model

At the anode,only two reactions occur; the formation of Oxygen from the dissociation of water

$$2H_2O - 4\ e^- \longrightarrow O_2(g) + 4\ H^+\ (aq) \qquad (i_5) \quad (2.35)$$

and the deposition of manganese dioxide ,from the manganese in solution

$$Mn^{2+}(aq) + 2H_2O - 2\ e^- \longrightarrow MnO_2(s) + 4\ H^+(aq) \qquad (i6) \quad (2.36)$$

The numbers in brackets $(i_5)$ and $(i_6)$ are their corresponding partial current densities.

The operation of the manganese electrowinning cell is made so as to minimize the production of manganese dioxide.To achieve this the anodic current density is usually set between 970 and 1500 A/m² (3).Under these conditions it is likely that the manganese dioxide reaction is mass transfer limited i.e.

$$i_6 = 2\ F\ k_6\ z_1 \qquad (2.37)$$

and

$$i_a = i_5 + i_6 \qquad (2.38)$$

The anodic current efficiency for the oxygen evolution will therefore be

$$\xi_a = \frac{i_5}{i_a} = 1 - \frac{i_6}{i_a} \qquad (2.39)$$

2.4.2 - Anodic Kinetic Model

At the anode,only two reactions occur; the formation of Oxygen from the dissociation of water

$$2H_2O - 4\ e^- \longrightarrow O_2(g) + 4\ H^+\ (aq) \qquad (i_5)\ (2.35)$$

and the deposition of manganese dioxide ,from the manganese in solution

$$Mn^{2+}(aq) + 2H_2O - 2\ e^- \longrightarrow MnO_2(s) + 4\ H^+(aq) \qquad (i6)\ (2.36)$$

The numbers in brackets ($i_5$) and ($i_6$) are their corresponding partial current densities.

The operation of the manganese electrowinning dell is made so as to minimize the production of manganese dioxide.To achieve this the anodic current density is usually set between 970 and 1500 A/m² (3).Under these conditions it is likely that the manganese dioxide reaction is mass transfer limited i.e.

$$i_6 = 2\ F\ k_6\ \xi_1 \qquad (2.37)$$

and

$$i_a = i_5 + i_6 \qquad (2.38)$$

The anodic current efficiency for the oxygen evolution will therefore be

$$\xi_a = \frac{i_5}{i_a} = 1 - \frac{i_6}{i_a} \qquad (2.39)$$

Stephen and Vogt(19) have developed a mass transfer correlation for gas evolving electrodes,which was shown by Bryson(14) to give limiting current density in the form

$$i_6 = \lambda_6 \, z_1 \, (i_5)^{0,5} \simeq \lambda_6 \, z_1 \, (i_a)^{0,5} \qquad (2.40)$$

Using the data from the Delta Manganese plant,the average anodic current efficiency is

$$\xi_a = 0,99 \qquad (2.41)$$

at $z_1 = 0,2$ and $i_a = 1000$ A/m²

Then using this set of conditions

$$\lambda_6 = 1,58$$

The equation modelling the anodic current efficiency $\xi_a$ is thus

$$\xi_a = 1 - 1,58 \, z_1 / (i_a)^{0,5} \qquad (2.42)$$

## 2.5 - The Cell Voltage Model

The cell voltage model is made up of three components,i.e. the cathodic potential,the anodic potential and the solution potential drop.These are respectively modelled by the following three equations

$$-E_c = -E^*_{01} + \frac{R\,T}{F} \ln \frac{i_1}{\gamma_1 \, i^*_{01}} \qquad (2.43)$$

$$E_a = E^*_{05} + \frac{R\,T}{F} \ln \frac{i_a}{z_2 \, i^*_{05}} \qquad (2.44)$$

$$\eta = \frac{L_c\, i}{K_c} + \frac{L_a\, i}{K_a} + \frac{d\, i}{K^* \varepsilon} \qquad (2.45)$$

The total cell voltage is thus:

$$V = - E_c + E_a + \eta \qquad (2.46)$$

Latimer(20) gives values for

$$E^*_{01} = -1{,}18 \text{ V} \quad \text{and} \quad E^*_{05} = 1{,}23 \text{ V} \qquad (2.47)$$

Hurlen and Valand(21) show that $i^*_{01}$ is a function of temperature which is given by

$$i^*_{01} = 7{,}1 \times 10^{10}\, T \exp\left(-\frac{63400}{R\,T}\right) \qquad (2.48)$$

where $i^*_{01}$ is the exchange current density at unit concentration for the manganese deposition reaction.

From studies on a lead anode Nicol(22) gives a value for current density on unit concentration for the oxygen evolution reaction as

$$i^*_{05} = 10^{-12} \text{ A/m}^3 \qquad (2.49)$$

## 2.6 - Water Vapour and Ammonia Losses

The hydrogen evolved at the cathode is assumed to be saturated with water vapour and to strip some ammonia from the solution so that the gas leaving the cathode compartment is in equilibrium with the gaseous ammonia species.The losses are calculated as follows

$$\frac{\text{moles of } H_2O \text{ lost from catholyte}}{\text{moles of } H_2 \text{ evolved}} = \frac{Y_0}{1 - Y_0 - Y_3} \qquad (2.50)$$

where $y_0$ = mole fraction of water
and $y_3$ = mole fraction of ammonia

Similarly for the calculation of the ammonia losses

$$\frac{\text{moles of } NH_3 \text{ lost from catholyte}}{\text{moles of } H_2 \text{ evolved}} = \frac{y_3}{1 - y_0 - y_3} \qquad (2.51)$$

From the anolyte, as there is no ammonia species present in the solution due to the anolyte solution equilibria, there are only water losses to consider from the oxygen evolution reaction. It has the same form as the previous equations and is

$$\frac{\text{moles of } H_2O \text{ lost from anolyte}}{\text{moles of } O_2 \text{ evolved}} = \frac{z_0}{1 - z_0} \qquad (2.52)$$

where $z_0$ is the mole fraction of water in the anolyte.

From steam tables (23) the following correlation was fitted to the data (please see Appendix G)

$$y_0 = -1,267 + 0,00428\ T \qquad (2.53)$$

for the range $310 < T < 320$

This same equation is used for $z_0$.

For the ammonia equilibrium it is assumed that Henry's law applies, thus $y_3$ should be proportional to $Y_3$. Using data from Perry(24), the proportionality constant is far lower than that calculated from plant data. The difference is most probably due to the reaction suggested by Gamali and Stender as reported by Louis and Martin (6)

$$NH_4^+ + e^- \rightleftharpoons H_{ads} + NH_3 \qquad (2.54)$$

If this reaction occurs to any significant extent, more free ammonia will be available in solution, increasing the amount of ammonia losses from the catholyte. The equation used in this model is that which best represents the observed ammonia losses on the Delta plant, i.e.

$$Y_3 = 2{,}16\ Y_3 \tag{2.55}$$

## 2.7 - Mass Balance

The feed composition is usually given in terms of $X_m$, $X_a$ and pH ; i.e. the total manganese , total ammonia present in the solution and its pH. Using the equilibrium ratio equations (2.2) , (2.4) and (2.6) and replacing $Y_j$ by $X_j$, the aqueous species concentrations $X_1$, $X_2$ , $X_3$ , $X_4$ and $X_5$ can be evaluated using the method demonstrated in Appendix B. $X_6$ is determined by the electrical neutrality equation

$$2\,X_1 + X_2 + X_3 + 2\,X_4 - 2\,X_6 = 0 \tag{2.56}$$

Once the various species concentrations are determined for the feed solution, an overall mass balance is performed to evaluate the anodic species concentrations and flows. The total mass balance as well as component balances are done to obtain the various concentrations.

The overall mass balance is performed as follows

$$\rho_f\, Q_f = \rho_a\, Q_a + P_{Mn} + P_{H_2} + P_{O_2} + P_{MnO_2} + L_{H_2Oc} + L_{H_2Oa} + L_{NH_3} \tag{2.57}$$

where $P_i$ stands for the production rates of the various components i and $L_i$ for the losses of ammonia and water. The equations for the losses are given by (2.50), (2.51) and (2.52). The production rate equations are given by

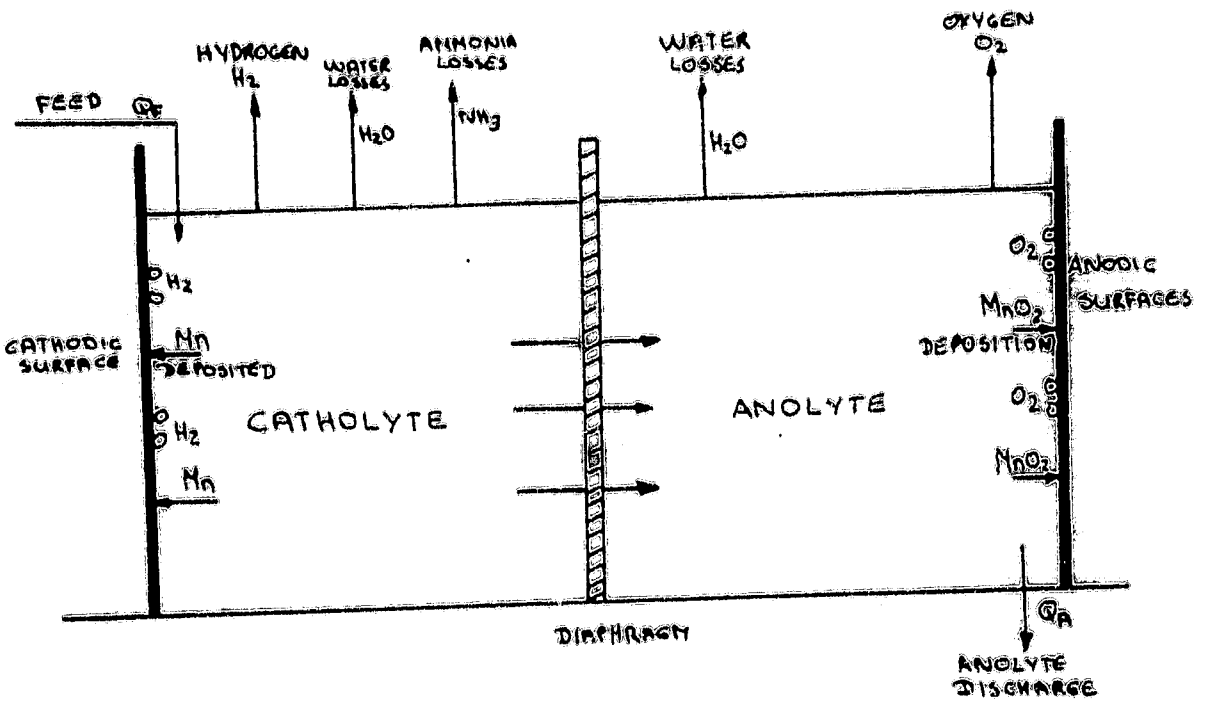


FIGURE 13 - Flow Diagram for Mass Balance

$$P_{Mn} = \frac{\xi_c \; I}{2 \quad F} \times 54,94 \times 10^{-3} \qquad (2.58)$$

$$P_{H_2} = \frac{(1 - \xi_c) \; I}{2 \quad F} \times 2,016 \times 10^{-3} \qquad (2.59)$$

$$P_{O_2} = \frac{\xi_a \; I}{4 \quad F} \times 31,999 \times 10^{-3} \qquad (2.60)$$

$$P_{MnO_2} = \frac{(1 - \xi_a) \; I}{4 \quad F} \times 86,939 \times 10^{-3} \qquad (2.61)$$

all in kg/s, where I is the total current through the cell in Amperes and F the Faradays' constant(96500 C $s^{-1}$).

Equation (2.57) will give the anolyte discharge in flow units.To estimate the component concentrations,individual mass balance equations are written for total manganese, total ammonia and total sulphate.These results together with the equilibrium ratio equation (2.9) and the electrical neutrality equation

$$2 z_1 + z_2 + z_3 - 2 z_6 - z_7 = 0 \qquad (2.62)$$

give the individual species concentrations,as shown in Appendix B.

The most important variable here is the anolyte pH,given as a function of $z_2$.To determine the equilibrium ratios for the necessary cathodic and anodic chemical reactions of interest,it was necessary to determine the temperatures of the various compartments ,which is explained in the next chapter (2.8).

Once the catholyte temperature is determined,the catholyte conditions are determined using the diaphragm model and the equilibrium ratio equations (2.2),(2.4)and (2.6).The diaphragm model equation (2.13) is used to calculate $Y_a$ and $W_2$ with $Y_2 \simeq 0$.The cathode kinetic model is then used to determine the actual value of $Y_2$ such that the hydrogen ions migrating through the diaphragm balance those used to produce $H_2$ and to react with $MnNH_3^{2+}$ and $NH_3$ according to the equations (2.1)and (2.3)

$$NH_3 + H^+ \rightleftharpoons NH_4^+ \qquad (2.3)$$

$$MnNH_3^{2+} + H^+ \rightleftharpoons Mn^{2+} + NH_4^+ \qquad (2.1)$$

The concentration $Y_m$ is taken to be approximately equal to $Z_m$ and thus the various species concentrations are determined using equations (2.2), (2.4) and (2.6) and the electrical neutrality equation

$$2\,Y_1 + Y_2 + Y_3 + 2\,Y_4 - 2\,Y_6 = 0 \qquad (2.63)$$

as shown in Appendix B.

## 2.8 - Energy Balance

The overall energy balance in kJ/s may be written as:

$$Q_f \,\Sigma\, X_j\, H_j + V\, I/1000 = Q_d\, \Sigma\, Z_j\, H_j + \Sigma\, M_j\, H_j + q_c + q_l \qquad (2.64)$$

The molar enthalpies can be expressed as :

$$H_j = \Delta H^{\circ}_{fj} + \int_{298}^{T} C^{\circ}_{pj}\, dT + \Delta H_{tj} + \Delta H^{1}_{j} \qquad (2.65)$$

The temperature range of normal cell operation is relatively close to 298K and since very little data is available for some of the aqueous species, the molar enthalpies will be approximated by

$$H_j = \Delta H^{\circ}_{fj} + (T - 298)\, C^{*}_{pj} \qquad (2.66)$$

The data used has been compiled from references (25), (26) and (27) and are listed in Table 5.

TABLE 5 - Molar Enthalpies of Formation and Molar Specific Heats

| Component | $\Delta H_f^o$ (kJ/kmole) x $10^{-4}$ | $C_p^*$ (kJ/kmole.K) |
|---|---|---|
| $H_2O$ (aq) | -25,58 | 75 |
| $Mn^{2+}$ (aq) | -22,05 | 184 |
| $H^+$ (aq) | 0,00 | 0 |
| $NH_4^+$ (aq) | -13,26 | 117 |
| $MnNH_3^{2+}$ (aq) | -30,08@ | 151@ |
| $NH_3$ (aq) | -8,03 | -34 |
| $SO_4^{2-}$ (aq) | -90,92 | -301 |
| $HSO_4^{2-}$ (aq) | -88,87 | -71 |
| $H_2O$ (g) | -24,18 | 34 |
| Mn (s) | 0,00 | 34 |
| $MnO_2$ (s) | -52,01 | 50 |
| $NH_3$ (g) | -4,60 | 34 |
| $O_2$ (g) | 0,00 | 34 |
| $H_2$ (g) | 0,00 | 34 |

@ - Values estimated from data for $Mn^{2+}$(aq) and $NH_3$(aq).

The energy removed by the cooling coils is

$$q_c = U A_c \Delta T = 4184\ Q_c (T_2 - T_1) \qquad (2.67)$$

where

$$\Delta T = \frac{T_2 - T_1}{\ln \frac{(T_a - T_1)}{(T_a - T_2)}} \qquad (2.68)$$

$q_1$ is the energy correction term due to losses to the surroundings, inaccuracies in the data and other factors such as neglecting heats of mixing. As a first guess this can be estimated at about 5% of the electrical energy input.

The energy balance permits $T_a$ and $T_2$ to be evaluated for a given $Q_c$ and $T_1$. On the other hand if $T_a$ is to be controlled at some required level, it will determine the values of $Q_c$ and $T_2$ for a given $T_1$. The catholyte temperature depends on $T_a$, $T_f$ and the energy transfer mechanisms in the diaphragms. It is found however, that the following empirical relation adequately models this variable

$$T_c = 0,7\ T_f + 0,3\ T_a \qquad (2.69)$$

Typical energy balance calculations are presented in Appendix C

## 3. RESULTS AND CASE STUDIES

### 3.1 - Typical Results - Discussion

A typical set of results using the model is shown on Table 6 below.By varying the input conditions it is found that a feed temperature of 39°C and a cathodic current density of 555 A/m² maximizes the current efficiency for manganese recovery.

TABLE 6 - Typical Model Results

Total Current = 56000 A ; Cell Voltage = 6,52 V
$i_c$ = 556A/m² ; $i_a$ = 1000A/m² ; $\xi_a$ = 0.990 ; $\xi_c$ = =0,702
$Q_c$ = 30,05 m³/hr ; $q_1$ = 18kJ/s ; $T_1$ = 292 K ; $T_2$ = 306 K

| Property | Feed | Catholyte | Anolyte |
|---|---|---|---|
| Flowrate (m³/s) | 0,000552 | - | 0,000549 |
| density (kg/m³) | 1185 | 1165 | 1160 |
| Temperature (°C) | 39,0 | 40,0 | 42,5 |
| Total Mn (kg/m³) | 32,16 | - | 11,48 |
| Total $NH_3$ (kg/m³) | 28,57 | - | 27,80 |
| pH | 6,88 | 7,60 | 0.64 |
| $Mn^{2+}$ (kmole/m³) | 0,534 | 0,131 | 0,209 |
| $NH_4^+$ (kmole/m³) | 1,611 | 1,785 | 1,635 |
| $MnNH_3^{2+}$ (kmole/m³) | 0,051 | 0,077 | - |
| $NH_3$ (kmole/m³) | 0,018 | 0,110 | - |
| $SO_4^{2-}$ (kmole/m³) | 1,391 | 1,098 | 0,883 |
| $HSO_4^-$ (kmole/m³) | - | - | 0,515 |
| $H_2O$ (kmole/m³) | 54,951 | - | 54,672 |

Based on this set of results, a typical Mass and Energy balance calculation is shown in Appendices B and C respectively.A catholyte pH of 7,6 maximizes the efficiency prior to the manganese hydroxide precipitation.This would occur at a pH of 7,64.

## 3.2 - Case Studies

By varying the input parameters to the computer model , the effect of certain parameters on the fractional cathode current efficiency was studied.These are presented and discussed and compared to previous available information.

### 3.2.1 - The Effect of Feed Flowrate on Fractional Current Efficiency

Figure 14 demonstrates the effect of altering the feed flowrate,using the values presented on Table 7.The curve is fairly steep ,which suggests that it may be profitable to exercise a high degree of control of this variable , particularly as the formation of $Mn(OH)_2$ at higher flowrates could result in extremely poor performance.

TABLE 7 - Fractional Current Efficiency versus Feed Flowrate

| Fractional current Efficiency | Feed Flowrate ($m^3/s$) x $10^3$ |
|---|---|
| 0,425 | 4,00 |
| 0,480 | 4,20 |
| 0,530 | 4,40 |
| 0,575 | 4,60 |
| 0,610 | 4,80 |
| 0.640 | 5,00 |
| 0,665 | 5,20 |
| 0,690 | 5,40 |
| 0,710 | 5,60 |
| 0,725 | 5,80 |
| 0,745 | 6,00 |

**Author** Rodrigues J C P
**Name of thesis** Modelling the performance of Manganese Eletrowinning cells 1983

***PUBLISHER:***
**University of the Witwatersrand, Johannesburg**
**©2013**

***LEGAL NOTICES:***

**Copyright Notice:** All materials on the University of the Witwatersrand, Johannesburg Library website are protected by South African copyright law and may not be distributed, transmitted, displayed, or otherwise published in any format, without the prior written permission of the copyright owner.

**Disclaimer and Terms of Use:** Provided that you maintain all copyright and other notices contained therein, you may download material (one machine readable copy and one print copy per page) for your personal and/or educational non-commercial use only.

The University of the Witwatersrand, Johannesburg, is not responsible for any errors or omissions and excludes any and all liability for any errors in or omissions from the information on the Library website.